Dalton Transactions

PAPER

View Article Online
View Journal | View Issue

Cite this: *Dalton Trans.*, 2014, **43**, 5343

Green-emitting iridium(III) complexes containing sulfanyl- or sulfone-functionalized cyclometallating 2-phenylpyridine ligands†

Edwin C. Constable,* Cathrin D. Ertl, Catherine E. Housecroft* and Jennifer A. Zampese

Received 25th December 2013,
Accepted 2nd February 2014

DOI: 10.1039/c3dt53626b

www.rsc.org/dalton

A series of $[Ir(C^N)_2(bpy)][PF_6]$ complexes in which the cyclometallating ligands contain fluoro, sulfane or sulfone groups is reported. The conjugate acids of the C^N ligands in the complexes are 2-(4-fluorophenyl)pyridine (H**1**), 2-(4-methylsulfonylphenyl)pyridine (H**3**), 2-(4-^{t}butylsulfanylphenyl)pyridine (H**4**), 2-(4-^{t}butylsulfonylphenyl)pyridine (H**5**), 2-(4-^{n}dodecylsulfanylphenyl)pyridine (H**6**), 2-(4-^{n}dodecylsulfonylphenyl)pyridine (H**7**). The single crystal structures of H**3** and H**5** are described. $[Ir(C^N)_2(bpy)][PF_6]$ with C^N = **1**, **3**, **4**, **5** and **7** were prepared from the appropriate $[Ir_2(C^N)_4Cl_2]$ dimer and bpy; the structure of $[Ir_2(\mathbf{3})_4Cl_2]\cdot 2CH_2Cl_2$ was determined. $[Ir(\mathbf{6})_2(bpy)][PF_6]$ was prepared by nucleophilic substitution starting from $[Ir(\mathbf{1})_2(bpy)][PF_6]$. The $[Ir(C^N)_2(bpy)][PF_6]$ complexes have been characterized by NMR, IR, absorption and emission spectroscopic and mass spectrometric methods. The single crystal structures of enantiomerically pure Δ-$[Ir(\mathbf{1})_2(bpy)][PF_6]$ and of *rac*-4{$[Ir(\mathbf{1})_2(bpy)][PF_6]$}·$Et_2O\cdot 2CH_2Cl_2$ are described, and the differences in inter-cation packing in the structures compared. $[Ir(\mathbf{1})_2(bpy)][PF_6]$, $[Ir(\mathbf{4})_2(bpy)][PF_6]$ and $[Ir(\mathbf{6})_2(bpy)][PF_6]$ (fluoro and sulfane substituents) are yellow emitters (λ_{em}^{max} between 557 and 577 nm), and the room temperature solution emission spectra are broad. The sulfone derivatives $[Ir(\mathbf{3})_2(bpy)][PF_6]$, $[Ir(\mathbf{5})_2(bpy)][PF_6]$ and $[Ir(\mathbf{7})_2(bpy)][PF_6]$ are green emitters and the emission spectra are structured (λ_{em}^{max} = 493 and 523 to 525 nm). High photoluminescence quantum yields (PLQYs) of 64–74% are observed for the sulfone complexes in degassed solutions. The emission lifetimes for the three complexes containing sulfone substituents are an order of magnitude longer (2.33 to 3.36 μs) than the remaining complexes (0.224 to 0.528 μs). Emission spectra of powdered solid samples have also been recorded; the broad emission bands have values of λ_{em}^{max} in the range 532 to 558 nm, and PLQYs for the powdered compounds are substantially lower (≤23%) than in solution. Trends in the redox potentials for the $[Ir(C^N)_2(bpy)][PF_6]$ complexes are in accord with the observed emission behaviour.

Introduction

Iridium(III) $[Ir(C^N)_2(N^N)]^+$ complexes incorporating cyclometallating (C^N) and *N*,*N*-chelating (N^N) ligands offer an adaptable family of emissive ionic materials for use in light-emitting electrochemical cells (LECs).[1–4] In $[Ir(C^N)_2(N^N)]^+$ cations, the localization of the HOMO and LUMO on the iridium/C^N domain and on the N^N ligands respectively, facilitates manipulation of the HOMO–LUMO separation by judicious choice of ligand substituents. Stabilization of the HOMO has been achieved by introducing electron-withdrawing substituents onto the C^N ligands, and 2-(2,4-difluorophenyl)pyridine (Hdfppy), and to a lesser extent 2-(4-fluorophenyl)pyridine, are regularly employed to achieve blue-shifted emissions in $[Ir(C^N)_2(N^N)]^+$ complexes.[1,5–7] Bolink, Frey and coworkers[8] have shown that the number (one or two) and positions of substitution of fluorine substituents in 2-phenylpyridine (Hppy) have little effect on the photophysical and electrochemical properties of $[Ir(C^N)_2(4,4'\text{-}^tBu_2bpy)][PF_6]$ complexes (4,4′-^{t}Bu$_2$bpy = 4,4′-di-*tert*-butyl-2,2′-bipyridine). However, significantly for application in LECs, increasing the number of fluorine atoms results in shorter lived LECs.

Less well explored than the use of fluoro-substituents is the incorporation of SR, SOR and SO_2R electron-withdrawing substituents, either for functionalization of the C^N[9–13] or N^N ligand.[14] Among these earlier studies is the use of 1-(4-(methylsulfonyl)phenyl)-1*H*-pyrazole (Hmsppz) as the cyclometallating ligand in a series of green emitting $[Ir(msppz)_2(N^N][PF_6]$ complexes which perform efficiently under bias in LECs.[13] The

Department of Chemistry, University of Basel, Spitalstrasse 51, CH-4056 Basel, Switzerland. E-mail: catherine.housecroft@unibas.ch

†CCDC 972690–972694. For crystallographic data in CIF or other electronic format see DOI: 10.1039/c3dt53626b

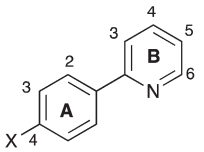

H1 X = F
H2 X = SMe
H3 X = SO_2Me
H4 X = S^{t}Bu
H5 X = $SO_2{}^t$Bu
H6 X = S^{n}C$_{12}$H$_{25}$
H7 X = $SO_2{}^n$C$_{12}$H$_{25}$

Scheme 1 Structures of the conjugate acids of the C^N ligands with labelling for NMR spectroscopic assignments.

achievement of both high luminances and efficiencies under low driving voltages[13] suggest that sulfone-functionalized cyclometallating ligands may be a viable alternative to the more commonly employed fluoro-substituted C^N ligands.

We present here a systematic study of the effects of functionalizing the cyclometallating Hppy ligand with increasingly electron-withdrawing substituents in the 4-position of the phenyl ring. Our aim was to apply the series of ligands shown in Scheme 1. Since the influence of fluoro-substituents is rather well understood, ligand H**1** was chosen to provide the benchmark complex $[Ir(\mathbf{1})_2(N\hat{}N)]^+$ to which to relate the properties of the sulfane and sulfone derivatized complexes. The increase in electron-withdrawing properties on changing from SMe and SO_2Me in compounds H**2** to H**3** (Scheme 1) is reflected in the different Hammett parameters (SMe, σ_m 0.15, σ_p 0.00; SO_2Me, σ_m 0.60, σ_p 0.72),[15–17] and one of us has observed that on going from $[Ru(tpy)_2]^{2+}$ to $[Ru(4'\text{-}MeO_2Stpy)_2]^{2+}$ (tpy = 2,2′:6′,2″-terpyridine, 4′-MeO_2Stpy = 4′-methylsulfonyl-2,2′:6′,2″-terpyridine), the sulfone unit causes a switch from a non-emissive complex in fluid solution to emissive behaviour in MeCN solution.[18] The pairs of ligands H**4**/H**5** and H**6**/H**7** were selected to investigate the added effects of introducing bulky (^{t}butyl) and long-chain (dodecyl) thiol and sulfone substituents.

Experimental

General

A Biotage Initiator 8 reactor was used for syntheses under microwave conditions.

^{1}H and ^{13}C spectra were recorded at 295 K on a Bruker Avance III-500 spectrometer; chemical shifts are referenced to residual solvent peaks with δ(TMS) = 0 ppm. Solution absorption spectra were recorded on an Agilent 8453 spectrophotometer, and FT-IR spectra on a Perkin Elmer Spectrum Two UATR instrument. Electrospray ionization (ESI) and MALDI-TOF mass spectra were recorded on Bruker esquire 3000^{plus} and Bruker Daltronics Microflex mass spectrometers, respectively. LC-ESI-MS employed a combination of Shimadzu (LC) and Bruker AmaZon X instruments. Electrochemical measurements were carried out using cyclic voltammetry and using a CH Instruments 900B potentiostat with glassy carbon working and platinum auxiliary electrodes; a silver wire was used as a pseudo-reference electrode. Solvent was dry, purified MeCN and 0.1 M $[^nBu_4N][PF_6]$ was used as supporting electrolyte. Cp_2Fe was used as internal reference and was added at the end of each experiment.

Solution emission spectra were recorded in MeCN on a Shimadzu 5301PC spectrofluorophotometer. Solution quantum yields were measured using a Hamamatsu absolute PL quantum yield spectrometer C11347 Quantaurus_QY. Lifetimes and emission spectra of powdered samples were measured using a Hamamatsu Compact Fluorescence lifetime Spectrometer C11367 Quantaurus-Tau.

Compound H**1** was prepared as reported in the literature[19] and the spectroscopic properties matched those reported.[20,21] $[Ir_2(COD)_2Cl_2]$[22] (COD = cycloocta-1,5-diene) and $[Ir_2(\mathbf{1})_4Cl_2]$[6] were prepared according to literature methods. All solvents were dried before use. Silica and alumina were purchased from Fluka (silica gel 60, 0.040–0.063 mm and activated, neutral aluminium oxide).

Compound H2. Compound H**2** has been previously reported[23] but the following procedure gives a higher yield. Compound H**1** (617 mg, 3.56 mmol) and an excess of NaSMe (1.06 g, 14.3 mmol) were added to *N*-methyl-2-pyrrolidone (NMP) (18 mL) in a microwave vial. The violet reaction mixture was heated at 80 °C for 1 h in a microwave reactor to give a dark brown suspension. This was poured into a mixture of H_2O and brine (3 : 1, 100 mL). The resulting yellow precipitate was separated by filtration, dissolved in CH_2Cl_2 and dried over Na_2SO_4. The solvent was removed under reduced pressure to yield H**2** as a yellow solid (0.665 g, 3.30 mmol, 92.7%). M.p. 59.5 °C. ^{1}H NMR (500 MHz, $CDCl_3$) δ/ppm 8.67 (ddd, J = 4.9, 1.9, 1.0 Hz, 1H, H^{B6}), 7.93 (m, 2H, H^{A2}), 7.76–7.67 (overlapping m, 2H, H^{B3+B4}), 7.34 (m, 2H, H^{A3}), 7.21 (ddd, J = 7.3, 4.8, 1.4 Hz, 1H, H^{B5}), 2.53 (s, 3H, H^{Me}). $^{13}C\{^1H\}$ NMR (126 MHz, $CDCl^3$) δ/ppm 157.0 (C^{B2}), 149.8 (C^{B6}), 139.9 (C^{A4}), 136.9 (C^{B4}), 136.2 (C^{A1}), 127.3 (C^{A2}), 126.5 (C^{A3}), 122.1 (C^{B5}), 120.2 (C^{B3}), 15.7 (C^{Me}). IR (solid, ν/cm^{-1}) 3086 (w), 3046 (w), 3002 (w), 2981 (w), 2919 (w), 1982 (w), 1910 (w), 1767 (w), 1661 (w), 1605 (w), 1583 (s), 1569 (s), 1552 (m), 1498 (w), 1458 (s), 1431 (s), 1399 (m), 1322 (w), 1296 (w), 1256 (w), 1227 (w), 1190 (m), 1154 (w), 1121 (w), 1098 (m), 1089 (m), 1057 (w), 1008 (m), 988 (m), 969 (w), 958 (m), 884 (w), 830 (m), 772 (s), 738 (s), 725 (m), 708 (m), 675 (w), 636 (w), 616 (w), 569 (w), 544 (w), 484 (m), 461 (m). ESI-MS m/z 202.0 $[M + H]^+$ (calc. 202.1). Found C 71.43, H 5.57, N 6.75; $C_{12}H_{11}NS$ requires C 71.60, H 5.51, N 6.96%.

Compound H3. Compound H**2** (1.00 g, 4.97 mmol) and sodium tungstate dihydrate (819 mg, 2.48 mmol) were dissolved in MeOH (35 mL). H_2O_2 (30%, 1.20 mL, 1.36 g) was added and the mixture was stirred overnight at room temperature. The suspension was poured into a mixture of H_2O and brine (3 : 1, 200 mL) and extracted with CH_2Cl_2 (3 × 100 mL). The combined organic phases were dried over Na_2SO_4 and the solvent was removed under reduced pressure to yield H**3** as a white powder (1.14 g, 4.89 mmol, 98.4%). M.p. 134.5 °C. ^{1}H NMR (500 MHz, $CDCl_3$) δ/ppm 8.75 (ddd, J = 4.7, 1.8, 1.0 Hz, 1H, H^{B6}), 8.21 (m, 2H, H^{A2}), 8.10–7.99 (m, 2H, H^{A3}), 7.87–7.75 (m, 2H, H^{B3+B4}), 7.34 (ddd, J = 7.0, 4.8, 1.6 Hz, 1H, H^{B5}), 3.09 (s, 3H, H^{Me}). $^{13}C\{^1H\}$ NMR (126 MHz, $CDCl_3$) δ/ppm 155.4 (C^{B2}), 150.2 (C^{B6}), 144.7 (C^{A1}), 140.7 (C^{A4}), 137.3 (C^{B4}),

128.0 (C^{A3}), 127.9 (C^{A2}), 123.5 (C^{B5}), 121.3 (C^{B3}), 44.7 (C^{Me}). IR (solid, ν/cm^{-1}) 3000 (w), 2921 (w), 1586 (m), 1563 (w), 1465 (m), 1435 (m), 1392 (w), 1314 (w), 1292 (s), 1185 (w), 1146 (s), 1087 (m), 1030 (w), 1013 (w), 988 (w), 964 (m), 848 (m), 789 (m), 776 (s), 750 (s), 677 (m), 636 (w), 616 (m), 562 (m), 548 (s), 514 (s). ESI-MS m/z 234.0 $[M + H]^+$ (calc. 234.1). Found: C 62.03, H 4.95, N 6.29; $C_{12}H_{11}NO_2S$ requires C 61.78, H 4.75, N 6.00%.

Compound H4. NaH (60% suspension in mineral oil, 235 mg, 5.88 mmol) was suspended in DMF (8 mL) under N_2. 2-Methyl-2-propanethiol (0.660 mL, 528 mg, 5.80 mmol) was added leading to gas evolution and a white foam. After the reaction mixture had been stirred for 10 min at room temperature, H**1** (501 mg, 2.89 mmol) was added with DMF (2 mL). The mixture was heated at 120 °C for 24 h. The yellow-orange solution was allowed to cool to room temperature and was then poured into water–brine (3 : 1, 50 mL). The resulting suspension was stirred for 5 min. The precipitate was separated by filtration, washed with H_2O and dried under vacuum. H**4** was isolated as a pale brown solid (704 mg, 2.89 mmol, 100%). M.p. 90.7 °C. ^{1}H NMR (500 MHz, $CDCl_3$) δ/ppm 8.70 (ddd, J = 4.8, 1.9, 1.1 Hz, 1H, H^{B6}), 7.95 (m, 2H, H^{A2}), 7.82–7.70 (overlapping m, 2H, H^{B3+B4}), 7.64 (m, 2H, H^{A3}), 7.26 (m, 1H, H^{B5}), 1.32 (s, 9H, H^{tBu}). $^{13}C\{^1H\}$ NMR (126 MHz, $CDCl_3$) δ/ppm 157.0 (C^{B2}), 149.9 (C^{B6}), 139.8 (C^{A1}), 137.9 (C^{A3}), 137.0 (C^{B4}), 133.9 (C^{A4}), 127.0 (C^{A2}), 122.5 (C^{B5}), 120.8 (C^{B3}), 46.4 (C^{CtBu}), 31.2 (C^{tBu}); IR (solid, ν/cm^{-1}) 1462 (m), 1429 (m), 1391 (w), 1366 (m), 1305 (w), 1289 (w), 1259 (w), 1168 (m), 1152 (m), 1098 (m), 1059 (w), 1031 (w), 1014 (m), 989 (m), 934 (w), 899 (w), 844 (s), 780 (s), 748 (s), 725 (m), 682 (w), 633 (w), 618 (w), 579 (w), 560 (m), 520 (m), 491 (m). ESI-MS m/z 244.0 $[M + H]^+$ (calc. 244.1). Found C 74.04, H 7.01, N 5.64; required for $C_{15}H_{17}NS$ C 74.03, H 7.04, N 5.76%.

Compound H5. H**4** (501 mg, 2.06 mmol) and sodium tungstate dihydrate (352 mg, 1.07 mmol) were dissolved in MeOH (13 mL). H_2O_2 (30%, 0.500 mL, 568 mg, 5.01 mmol) was added and the suspension was stirred at room temperature for 20 h. CH_2Cl_2 (100 mL) was then added and the white precipitate was separated by filtration. The filtrate was washed with H_2O (50 mL), the aqueous layer extracted with CH_2Cl_2 (100 mL) and the combined organic layers dried over Na_2SO_4. The solvent was removed under reduced pressure and the residue was purified by column chromatography (silica, CH_2Cl_2 with 1% MeOH). H**5** was isolated as a white powder (473 mg, 1.72 mmol, 83.5%). M.p. 174.4 °C. ^{1}H NMR (500 MHz, $CDCl_3$) δ/ppm 8.75 (ddd, J = 4.7, 1.8, 1.1 Hz, 1H, H^{B6}), 8.17 (m, 2H, H^{A2}), 7.98 (m, 2H, H^{A3}), 7.88–7.75 (overlapping m, 2H, H^{B3+B4}), 7.33 (ddd, J = 6.7, 4.8, 1.7 Hz, 1H, H^{B5}), 1.37 (s, 9H, H^{tBu}). $^{13}C\{^1H\}$ NMR (126 MHz, $CDCl_3$) δ/ppm 155.7 (C^{B2}), 150.2 (C^{B6}), 144.5 (C^{A1}), 137.3 (C^{B4}), 135.5 (C^{A4}), 131.1 (C^{A3}), 127.3 (C^{A2}), 123.5 (C^{B5}), 121.3 (C^{B3}), 60.1 (C^{CtBu}), 23.8 (C^{tBu}). IR (solid, ν/cm^{-1}) 2970 (w), 1586 (m), 1561 (w), 1463 (m), 1436 (w), 1395 (w), 1314 (w), 1287 (s), 1192 (w), 1159 (w), 1131 (s), 1113 (m), 1079 (s), 1011 (m), 990 (w), 853 (m), 801 (w), 778 (s), 752 (w), 741 (w), 722 (m), 694 (s), 646 (s), 616 (m), 579 (s), 555 (m), 517 (m), 505 (m). ESI-MS m/z 276.0 $[M + H]^+$ (calc. 276.1). Found C 65.41, H 6.31, N 5.14; $C_{15}H_{17}NO_2S$ requires C 65.43, H 6.22, N 5.09%.

Compound H6. NaH (60% suspension in mineral oil, 187 mg, 4.67 mmol) was suspended in DMF (6 mL) under N_2. 1-Dodecanethiol (1.14 mL, 956 mg, 4.63 mmol) and then DMF (4 mL) were added and the mixture was stirred for 10 min. H**1** (400 mg, 2.31 mmol) was added with DMF (2 mL) and the mixture was heated at 120 °C for 4 h. The yellow mixture was allowed to cool to room temperature and was then poured into water–brine (3 : 1, 50 mL). The resulting suspension was stirred for 5 min and the precipitate was removed by filtration, washed with H_2O, dried under vacuum and purified by column chromatography (silica, n-hexane–EtOAc 6 : 1 by vol. changing to 2 : 1). H**6** was isolated as a white solid (542 mg, 1.52 mmol, 65.8%). M.p. 65.3 °C. ^{1}H NMR (500 MHz, $CDCl_3$) δ/ppm 8.67 (ddd, J = 4.8, 1.8, 1.0 Hz, 1H, H^{B6}), 7.91 (m, 2H, H^{A2}), 7.78–7.63 (overlapping m, 2H, H^{B3+B4}), 7.39 (m, 2H, H^{A3}), 7.21 (ddd, J = 7.2, 4.8, 1.4 Hz, 1H, H^{B5}), 2.97 (m, 2H, H^{SCH2}), 1.68 (m, 2H, $H^{SCH2CH2}$), 1.43 (m, 2H, $H^{SCH2CH2CH2}$), 1.35–1.12 (overlapping m, 16H, H^{CH2}), 0.88 (t, J = 6.9 Hz, 3H, H^{CH3}). $^{13}C\{^1H\}$ NMR (126 MHz, $CDCl_3$) δ/ppm 157.0 (C^{B2}), 149.8 (C^{B6}), 138.7 (C^{A4}), 136.9 (C^{B4}), 136.7 (C^{A1}), 128.6 (C^{A3}), 127.3 (C^{A2}), 122.1 (C^{B5}), 120.3 (C^{B3}), 33.3 (C^{SCH2}), 32.1 (C^{CH2}), 29.8 ($2C^{CH2}$), 29.7 ($2C^{CH2}$), 29.5 (C^{CH2}), 29.3 (C^{CH2}), 29.2 ($C^{SCH2CH2}$), 29.0 ($C^{SCH2CH2CH2}$), 22.8 (C^{CH2}), 14.3 (C^{CH3}). IR (solid, ν/cm^{-1}) 3059 (w), 3003 (w), 2954 (m), 2917 (s), 2872 (m), 2850 (s), 1585 (s), 1571 (m), 1554 (w), 1496 (w), 1463 (s), 1432 (s), 1398 (w), 1379 (m), 1297 (m), 1259 (w), 1242 (w), 1191 (w), 1153 (w), 1122 (w), 1100 (m), 1056 (w), 1009 (m), 988 (w), 834 (m), 768 (s), 734 (m), 720 (m), 708 (m), 636 (w), 616 (w), 548 (w), 513 (w), 488 (w), 462 (m). MALDI-TOF MS (no matrix) m/z 355.7 $[M]^+$ (calc. 355.2). Found C 77.75, H 9.76, N 4.05; $C_{23}H_{33}NS$ requires C 77.69, H 9.35, N 3.94%.

Compound H7. H**6** (212 mg, 0.597 mmol) and sodium tungstate dihydrate (98.4 mg, 0.298 mmol) were suspended in MeOH (15 mL). H_2O_2 (35%, 0.120 mL, 136 mg, 1.40 mmol) was added and the mixture was stirred at room temperature overnight. Water (50 mL) was added and the suspension was stirred for 15 min, after which time the precipitate was separated by filtration. It was washed with H_2O and dried under vacuum. H**7** was isolated as a white solid (207 mg, 0.534 mmol, 89.4%). M.p. 84.4 °C. ^{1}H NMR (500 MHz, $CDCl_3$) δ/ppm 8.74 (ddd, J = 5.0, 1.3 Hz, 1H, H^{B6}), 8.19 (m, 2H, H^{A2}), 8.00 (m, 2H, H^{A3}), 7.81 (m, 2H, H^{B3+B4}), 7.33 (ddd, J = 6.7, 4.7, 1.6 Hz, 1H, H^{B5}), 3.11 (m, 2H, H^{SO2CH2}), 1.71 (m, 2H, $H^{SO2CH2CH2}$), 1.35 (m, 2H, $H^{SO2CH2CH2CH2}$), 1.31–1.18 (overlapping m, 16H, H^{CH2}), 0.87 (t, J = 7.0 Hz, 3H, H^{CH3}). $^{13}C\{^1H\}$ NMR (126 MHz, $CDCl_3$) δ/ppm 155.5 (C^{B2}), 150.2 (C^{B6}), 144.6 (C^{A1}), 139.3 (C^{A4}), 137.2 (C^{B4}), 128.7 (C^{A3}), 127.8 (C^{A2}), 123.5 (C^{B5}), 121.3 (C^{B3}), 56.6 (C^{SO2CH2}), 32.0 (C^{CH2}), 29.72 (C^{CH2}), 29.69 (C^{CH2}), 29.6 (C^{CH2}), 29.5 (C^{CH2}), 29.4 (C^{CH2}), 29.2 (C^{CH2}), 28.4 ($C^{SO2CH2CH2CH2}$), 22.9 ($C^{SO2CH2CH2}$), 22.8 (C^{CH2}), 14.3 (C^{CH3}). IR (solid, ν/cm^{-1}) 2915 (m), 2848 (m), 1586 (w), 1562 (w), 1468 (m), 1436 (w), 1399 (w), 1301 (m), 1285 (m), 1271 (m), 1144 (s), 1099 (w), 1086 (m), 1027 (w), 1009 (w), 991 (w), 853 (w), 776 (s), 758 (m), 739 (m), 722 (w), 691 (s),

635 (w), 621 (m), 606 (s), 557 (m), 528 (s), 496 (m). ESI-MS *m*/*z* 388.2 $[M + H]^+$ (calc. 388.2). Found C 71.30, H 8.79, N 3.77; $C_{23}H_{33}NO_2S$ requires C 71.27, H 8.58, N 3.61%.

$[Ir_2(3)_4Cl_2]$. $[Ir_2(COD)_2Cl_2]$ (285 mg, 0.424 mmol) and H**3** (395 mg, 1.69 mmol) were suspended in degassed 2-ethoxyethanol and the mixture purged with argon. The suspension was heated at reflux overnight and was then allowed to cool to room temperature. The yellow precipitate was separated by filtration, washed with H_2O and EtOH, and dried under vacuum. $[Ir_2(3)_4Cl_2]$ was isolated as a yellow powder (516 mg, 0.373 mmol, 88.0% crude) and was used without further purification. ^{1}H NMR (500 MHz, $CDCl_3$) δ/ppm 9.21 (ddd, J = 5.8, 1.6, 0.7 Hz, 4H, H^{B6}), 8.06 (ddd, J = 8.4, 1.4, 0.7 Hz, 4H, H^{B3}), 7.95 (ddd, J = 8.1, 7.5, 1.6 Hz, 4H, H^{B4}), 7.68 (d, J = 8.2 Hz, 4H, H^{A3}), 7.36 (dd, J = 8.1, 1.9 Hz, 4H, H^{A4}), 7.01 (ddd, J = 7.3, 5.7, 1.4 Hz, 4H, H^{B5}), 6.36 (d, J = 1.9 Hz, 4H, H^{A6}), 2.75 (s, 12H, H^{Me}). $^{13}C\{^1H\}$ NMR (126 MHz, $CDCl_3$) δ/ppm 166.5 (C^{B2}), 151.8 (C^{B6}), 149.2 (C^{A2}), 144.8 ($C^{A1/A5}$), 139.8 ($C^{A1/A5}$), 138.0 (C^{B4}), 128.1 (C^{A6}), 124.4 (C^{B5}), 124.3 (C^{A3}), 121.0 (C^{A4}), 120.6 (C^{B3}), 44.3 (C^{Me}). ESI-MS *m*/*z* 657.1 $[Ir(3)_2]^+$ (calc. 657.1), 698.2 $[Ir(3)_2(MeCN)]^+$ (calc. 698.1).

$[Ir_2(4)_4Cl_2]$. Compound H**4** (401 mg, 1.65 mmol) was dissolved in 2-ethoxyethanol (18 mL) in a vial and the solution purged with N_2. $[Ir_2(COD)_2Cl_2]$ (280 mg, 0.417 mmol) was added and the mixture heated at 110 °C for 1.5 h in a microwave reactor. The yellow precipitate was separated by filtration, washed with H_2O and EtOH and dried under vacuum to yield $[Ir_2(4)_4Cl_2]$ as a yellow solid (383 mg, 0.269 mmol, 64.5% crude). The compound was used without further purification. ^{1}H NMR (500 MHz, $CDCl_3$) δ/ppm 9.29 (d, J = 5.5 Hz, 4H, H^{B6}), 7.89 (d, J = 8.0 Hz, 4H, H^{B3}), 7.76 (*pseudo*-td, J = 7.8, 1.6 Hz, 4H, H^{B4}), 7.42 (d, J = 8.0 Hz, 4H, H^{A3}), 6.92 (dd, J = 7.9, 1.7 Hz, 4H, H^{A4}), 6.78 (ddd, J = 7.3, 5.7, 1.5 Hz, 4H, H^{B5}), 5.96 (d, J = 1.6 Hz, 4H, H^{A6}), 0.98 (s, 36H, H^{tBu}). ESI-MS *m*/*z* 677.2 $[Ir(4)_2]^+$ (calc. 677.2), 718.3 $[Ir(4)_2(MeCN)]^+$ (calc. 718.2).

$[Ir_2(5)_4Cl_2]$. Compound H**5** (151 mg, 0.548 mmol, 2.0 eq.) was suspended in 2-ethoxyethanol (3 mL) and H_2O (1 mL) under N_2 atmosphere. $IrCl_3{\cdot}nH_2O$ (≈82% $IrCl_3$, 99.2 mg, 1.0 eq.) was added and the suspension was heated at reflux for 21 h. The mixture was allowed to cool to room temperature and then H_2O was added. The precipitate was removed by filtration and was washed with H_2O to give $[Ir_2(5)_4Cl_2]$ as a yellow powder (101 mg, 0.0650 mmol, 48%). This was used without further purification. ^{1}H NMR (500 MHz, $CDCl_3$) δ/ppm 9.30 (ddd, J = 5.8, 1.5, 0.6 Hz, 4H, H^{B6}), 8.03 (ddd, J = 8.3, 1.3, 0.6 Hz, 4H, H^{B3}), 7.93 (td, J = 7.8, 1.5 Hz, 4H, H^{B4}), 7.64 (d, J = 8.2 Hz, 4H, H^{A3}), 7.30 (dd, J = 8.1, 1.7 Hz, 4H, H^{A4}), 6.98 (ddd, J = 7.3, 5.7, 1.5 Hz, 4H, H^{B5}), 6.21 (d, J = 1.8 Hz, 4H, H^{A6}), 1.00 (s, 36H, H^{tBu}). $^{13}C\{^1H\}$ NMR (126 MHz, $CDCl_3$) δ/ppm 166.7 (C^{B2}), 151.8 (C^{B6}), 148.9 (C^{A2}), 143.8 ($C^{A1/A5}$), 137.9 (C^{B4}), 134.4 ($C^{A5/A1}$), 131.6 (C^{A6}), 124.13 (C^{B5}), 124.07 (C^{A4}), 123.5 (C^{A3}), 120.5 (C^{B3}), 59.7 (C^{CtBu}), 23.5 (C^{tBu}). ESI-MS *m*/*z* 741.2 $[Ir(5)_2]^+$ (calc. 741.1), 782.1 $[Ir(5)_2(MeCN)]^+$ (calc. 782.2), 823.1 $[Ir(5)_2(MeCN)_2]^+$ (calc. 823.2).

$[Ir_2(7)_4Cl_2]$. $IrCl_3{\cdot}nH_2O$ (≈82% $IrCl_3$, 93.5 mg, 0.257 mmol) was added to a suspension of H**7** (200 mg, 0.516 mmol) in 2-ethoxyethanol (3 mL) and H_2O (1 mL) under N_2. The mixture was heated at reflux for 22 h. After cooling to room temperature, the mixture was poured into H_2O (≈50 mL) and stirred at room temperature for a few min. The resulting suspension was poured into brine (≈40 mL) and stirred again at room temperature. The precipitate was removed by filtration, washed with H_2O, EtOH and Et_2O and dried under vacuum. $[Ir_2(7)_4Cl_2]$ was isolated as a yellow powder (216 mg, 0.108 mmol, 84.0% crude) and was used without further purification. ^{1}H NMR (500 MHz, $CDCl_3$) δ/ppm 9.23 (ddd, J = 5.7, 1.5, 0.6 Hz, 4H, H^{B6}), 8.04 (*pseudo*-dt, J = 8.4, 1.0 Hz, 4H, H^{B3}), 7.94 (*pseudo*-td, J = 7.8, 1.6 Hz, 4H, H^{B4}), 7.66 (d, J = 8.2 Hz, 4H, H^{A3}), 7.31 (dd, J = 8.1, 1.8 Hz, 4H, H^{A4}), 6.99 (ddd, J = 7.3, 5.7, 1.5 Hz, 4H, H^{B5}), 6.30 (d, J = 1.8 Hz, 4H, H^{A6}), 2.74 (m, 8H, H^{SO2CH2}), 1.43 (m, 8H, $H^{SO2CH2CH2}$), 1.33–1.05 (overlapping m, 72H, H^{Me}), 0.88 ppm (t, J = 7.0 Hz, 12H, H^{Me}). $^{13}C\{^1H\}$ NMR (126 MHz, $CDCl_3$) δ/ppm 166.6 (C^{B2}), 151.8 (C^{B6}), 149.0 (C^{A2}), 144.7 ($C^{A1/A5}$), 138.6 ($C^{A5/A1}$), 137.9 (C^{B4}), 128.9 (C^{A6}), 124.3 (C^{B5}), 124.2 (C^{A3}), 121.6 (C^{A4}), 120.5 (C^{B3}), 56.2 (C^{SO2CH2}), 32.1 (C^{CH2}), 29.73 (C^{CH2}), 29.72 (C^{CH2}), 29.6 (C^{CH2}), 29.5 (C^{CH2}), 29.4 (C^{CH2}), 29.2 (C^{CH2}), 28.3 (C^{CH2}), 22.8 (C^{CH2}), 22.5 ($C^{SO2CH2CH2}$), 14.3 (C^{Me}). MALDI-TOF MS (no matrix) *m*/*z* 965.9 $[Ir(7)_2]^+$ (calc. 965.4).

$[Ir(1)_2(bpy)][PF_6]$. $[Ir_2(1)_4Cl_2]$ (350 mg, 0.306 mmol) and bpy (150 mg, 0.960 mmol) were suspended in MeOH (45 mL). The mixture was heated at reflux overnight and then allowed to cool to room temperature. After filtration, an excess of solid NH_4PF_6 was added to the filtrate and the mixture was stirred for 1 h at room temperature. The yellow precipitate was separated by filtration, washed with H_2O and redissolved in CH_2Cl_2. The solution was dried over Na_2SO_4 and the solvent removed under reduced pressure. The yellow residue was purified by column chromatography (silica, CH_2Cl_2 changing to CH_2Cl_2–2% MeOH). $[Ir(1)_2(bpy)][PF_6]$ was isolated as a yellow solid (405 mg, 0.483 mmol, 78.9%). ^{1}H NMR (500 MHz, CD_3CN) δ/ppm 8.53 (*pseudo*-dt, J = 8.3, 1.0 Hz, 2H, H^{E3}), 8.14 (*pseudo*-td, J = 8.0, 1.6 Hz, 2H, H^{E4}), 8.01 (m, 4H, H^{B3+E6}), 7.85 (m, 4H, H^{A3+B4}), 7.57 (ddd, J = 5.8, 1.5, 0.8 Hz, 2H, H^{B6}), 7.51 (ddd, J = 7.7, 5.5, 1.2 Hz, 2H, H^{E5}), 7.04 (ddd, J = 7.3, 5.8, 1.4 Hz, 2H, H^{B5}), 6.81 (m, 2H, H^{A4}), 5.89 (dd, J_{HF} = 9.6 Hz, J_{HH} = 2.6 Hz, 2H, H^{A6}). $^{13}C\{^1H\}$ NMR (126 MHz, CD_3CN) δ/ppm 167.1 (C^{B2}), 164.6 (d, J_{CF} = 253 Hz, C^{A5}), 156.6 (C^{E2}), 154.3 (d, J_{CF} = 5.8 Hz, C^{A1}), 151.8 (C^{E6}), 150.1 (C^{B6}), 141.4 (d, J_{CF} = 2.1 Hz, C^{A2}), 140.5 (C^{E4}), 139.8 (C^{B4}), 129.4 (C^{E5}), 128.1 (d_{CF}, J = 9.4 Hz, C^{A3}), 125.7 (C^{E3}), 124.5 (C^{B5}), 121.0 (C^{B3}), 118.3 (d_{CF}, J = 17.7 Hz, C^{A6}), 110.5 (d, J = 23.3 Hz, C^{A4}). IR (solid, ν/cm^{-1}) 1594 (m), 1568 (m), 1555 (m), 1482 (w), 1447 (m), 1434 (m), 1314 (w), 1262 (w), 1245 (w), 1187 (m), 1163 (w), 1032 (w), 833 (s), 766 (s), 733 (m), 675 (w), 576 (m), 556 (s). UV/Vis (MeCN, 1.1 × 10^{-5} mol dm^{-3}) λ/nm (ε/dm^3 mol^{-1} cm^{-1}) 251 (62 000), 264 (60 000), 295 sh (33 000), 310 sh (2000), 395 sh (4300). Emission (MeCN, 1.1 × 10^{-5} mol dm^{-3}, λ_{exc} = 269 nm) λ_{em}^{max} = 557 nm. ESI-MS *m*/*z* 693.2 $[M - PF_6]^+$ (calc. 693.1). Found C 45.95, H 2.84, N 6.74; $C_{32}H_{22}F_8IrN_4P$ requires C 45.88, H 2.65, N 6.69%.

$[Ir(3)_2(bpy)][PF_6]$. $[Ir_2(3)_4Cl_2]$ (109 mg, 0.0574 mmol) and bpy (26.9 mg, 0.172 mmol) were suspended in MeOH (10 mL)

and the mixture was heated at 120 °C in a microwave reactor for 1 h (15 bar). After cooling, an excess of solid NH_4PF_6 was added to the yellow solution and the resulting suspension was stirred for 15 min at room temperature. The yellow precipitate that formed was separated by filtration, was washed with MeOH and redissolved in CH_2Cl_2. The solvent was removed under reduced pressure and the product was purified by column chromatography (silica, CH_2Cl_2 changing to CH_2Cl_2–4% MeOH). The major fraction was collected and solvent removed under reduced pressure. The residue was suspended in CH_2Cl_2 and the mixture sonicated and then filtered. $[Ir(\mathbf{3})_2(bpy)][PF_6]$ was isolated as a yellow solid (92.3 mg, 0.0964 mmol, 84.0%). ^{1}H NMR (500 MHz, CD_3CN) δ/ppm 8.54 (*pseudo*-dt, J = 8.3, 1.1 Hz, 2H, H^{E3}), 8.23 (*pseudo*-dt, J = 8.2, 1.1 Hz, 2H, H^{B3}), 8.15 (*pseudo*-td, J = 8.0, 1.6 Hz, 2H, H^{E4}), 8.02 (d, J = 8.3 Hz, 2H, H^{A3}), 7.98 (ddd, J = 8.0, 7.7, 1.5 Hz, 2H, H^{B4}), 7.95 (ddd, J = 5.4, 1.6, 0.8 Hz, 2H, H^{E6}), 7.72 (ddd, J = 5.8, 1.5, 0.7 Hz, 2H, H^{B6}), 7.58 (dd, J = 8.3, 1.9 Hz, 2H, H^{A4}), 7.51 (ddd, J = 7.7, 5.5, 1.2 Hz, 2H, H^{E5}), 7.21 (ddd, J = 7.4, 5.8, 1.4 Hz, 2H, H^{B5}), 6.70 (d, J = 1.9 Hz, 2H, H^{A6}), 2.89 (s, 6H, H^{Me}). $^{13}C\{^1H\}$ NMR (126 MHz, CD_3CN) δ/ppm 166.2 (C^{B2}), 156.6 (C^{E2}), 152.0 (C^{E6}), 151.2 (C^{A1}), 150.9 (C^{B6}), 150.2 (C^{A2}), 142.3 (C^{A5}), 140.7 (C^{E4}), 140.3 (C^{B4}), 129.6 (C^{A6+E5}), 126.31 (C^{A3}), 126.29 (C^{B5}), 125.8 (C^{E3}), 122.6 (C^{A4}), 122.6 (C^{B3}), 44.3 (C^{Me}). IR (solid, ν/cm^{-1}) 2927 (w), 1608 (w), 1575 (w), 1475 (m), 1447 (w), 1430 (w), 1375 (w), 1294 (m), 1267 (w), 1144 (s), 1091 (m), 1062 (m), 1030 (w), 957 (m), 892 (w), 838 (s), 808 (m), 782 (m), 753 (s), 733 (m), 699 (m), 666 (w), 651 (w), 600 (w), 592 (w), 557 (s), 546 (s), 524 (m), 487 (s). UV/Vis (MeCN, 1.0×10^{-5} mol dm^{-3}) λ/nm (ε/dm^3 mol^{-1} cm^{-1}) 256 (58 000), 300 sh (30 000), 350 sh (7500), 390 (4900), 425 sh (3200). Emission (MeCN, 1.0×10^{-5} mol dm^{-3}, λ_{exc} = 262 nm) λ_{em}^{max} = 493, 525 nm. ESI-MS m/z 813.1 $[M - PF_6]^+$ (calc. 813.1). Found C 41.74, H 3.33, N 5.90; $C_{34}H_{28}F_6IrN_4O_4PS_2 \cdot H_2O$ requires C 41.84, H 3.10, N 5.74%.

$[Ir(\mathbf{4})_2(bpy)][PF_6]$. $[Ir_2(\mathbf{4})_4Cl_2]$ (144 mg, 0.101 mmol) and bpy (66.0 mg, 0.423 mmol) were suspended in MeOH (15 mL) and the mixture was heated at reflux for 16 h. The orange solution was allowed to cool to room temperature. An excess of solid NH_4PF_6 was added followed by enough H_2O to precipitate the product, and the resulting suspension was stirred for 10 min. The yellow precipitate was separated by filtration, washed with H_2O and MeOH and then redissolved in CH_2Cl_2. The solution was dried over Na_2SO_4 and the solvent was then removed under reduced pressure. The residue was purified twice by column chromatography (silica, CH_2Cl_2 changing to CH_2Cl_2 with 1% MeOH; alumina, CH_2Cl_2 changing to CH_2Cl_2–5% MeOH). The residue was dissolved in MeOH and an excess of solid NH_4PF_6 followed by H_2O were added. The resulting suspension was stirred for 5 min, and the yellow precipitate was collected by filtration and redissolved in CH_2Cl_2. The solution was dried over Na_2SO_4 and the solvent was removed *in vacuo*. $[Ir(\mathbf{4})_2(bpy)][PF_6]$ was isolated as a yellow solid (139 mg, 0.142 mmol, 70.3%). ^{1}H NMR (500 MHz, CD_3CN): δ/ppm 8.54 (*pseudo*-dt, J = 8.2, 1.0 Hz, 2H, H^{E3}), 8.15 (*pseudo*-td, J = 7.9, 1.6 Hz, 2H, H^{E4}), 8.07 (m, 4H, H^{B3+E6}), 7.86 (ddd, J = 8.2, 7.6, 1.5 Hz, 2H, H^{B4}), 7.72 (d, J = 8.0 Hz, 2H, H^{A3}), 7.61 (*pseudo*-dt, J = 5.8, 1.2 Hz, 2H, H^{B6}), 7.51 (ddd, J = 7.5, 5.3, 1.2 Hz, 2H, H^{E5}), 7.13 (dd, J = 8.0, 1.7 Hz, 2H, H^{A4}), 7.05 (ddd, J = 7.4, 5.8, 1.4 Hz, 2H, H^{B5}), 6.30 (d, J = 1.7 Hz, 2H, H^{A6}), 1.00 (s, 18H, H^{tBu}). $^{13}C\{^1H\}$ NMR (126 MHz, CD_3CN) δ/ppm 167.7 (C^{B2}), 156.7 (C^{E2}), 151.8 (C^{E6}), 150.9 (C^{A5}), 150.3 (C^{B6}), 145.2 (C^{B6}), 140.4 (C^{A2}), 140.3 (C^{E4}), 139.7 (C^{A6}), 136.0 (C^{B4}), 131.6 (C^{A1}), 129.4 (C^{A4}), 125.7 (C^{E3}), 125.5 (C^{A3}), 124.8 (C^{B5}), 121.3 (C^{B3}), 46.8 (C^{CtBu}), 31.1 (C^{tBu}). IR (solid, ν/cm^{-1}) 2970 (w), 1607 (m), 1569 (m), 1472 (m), 1447 (m), 1425 (m), 1366 (m), 1313 (w), 1258 (w), 1162 (m), 1099 (w), 1062 (w), 875 (w), 834 (s), 778 (s), 765 (s), 733 (m), 650 (w), 600 (w), 557 (s). UV/Vis (MeCN, 1.0×10^{-5} mol dm^{-3}) λ/nm (ε/dm^3 mol^{-1} cm^{-1}) 261 (57 000), 305 sh (35 000), 415 sh (4800). Emission (MeCN, 0.99×10^{-5} mol dm^{-3}, λ_{exc} = 260 nm): λ_{em}^{max} = 568 nm. ESI-MS m/z 833.5 $[M - PF_6]^+$ (calc. 833.2). Found C 48.96, H 4.35, N 5.70; $C_{40}H_{40}F_6IrN_4PS_2$ requires C 49.12, H 4.12, N 5.73%.

$[Ir(\mathbf{5})_2(bpy)][PF_6]$. $[Ir_2(\mathbf{5})_4Cl_2]$ (101 mg, 0.0650 mmol) and bpy (44.3 mg, 0.284 mmol) were suspended in MeOH (10 mL) and the mixture was heated at reflux for 14 h. The solution was left to cool to room temperature, and an excess of solid NH_4PF_6 was then added followed by enough H_2O to precipitate the product. The resulting suspension was stirred for 30 min. The yellow precipitate was separated by filtration, washed with H_2O and redissolved in CH_2Cl_2. After removal of the solvent under reduced pressure, the residue was purified by column chromatography (silica, CH_2Cl_2 changing to CH_2Cl_2–2% MeOH). $[Ir(\mathbf{5})_2(bpy)][PF_6]$ was isolated as a yellow solid (119 mg, 0.114 mmol, 87.7%). ^{1}H NMR (500 MHz, CD_3CN) δ/ppm 8.58 (dd, J = 8.2, 1.1 Hz, 2H, H^{E3}), 8.22 (d, J = 8.0 Hz, 2H, H^{B3}), 8.17 (*pseudo*-td, J = 8.0, 1.5 Hz, 2H, H^{E4}), 8.09 (m, 2H, H^{E6}), 8.02–7.93 (overlapping m, 4H, H^{A3+B4}), 7.71 (m, 2H, H^{B6}), 7.51 (ddd, J = 6.9, 5.5, 1.2 Hz, 2H, H^{E5}), 7.45 (dd, J = 8.2, 1.8 Hz, 2H, H^{A4}), 7.20 (ddd, J = 7.4, 5.8, 1.4 Hz, 2H, H^{B5}), 6.50 (d, J = 1.8 Hz, 2H, H^{A6}), 0.93 (s, 18H, H^{tBu}). $^{13}C\{^1H\}$ NMR (126 MHz, CD_3CN, 295 K) δ/ppm 166.2 (C^{B2}), 156.6 (C^{E2}), 152.3 (C^{E6}), 150.9 (C^{B6}), 150.6 ($C^{A1/A5}$), 150.1 (C^{A2}), 140.8 (C^{E4}), 140.4 (C^{B4}), 135.9 ($C^{A5/A1}$), 133.2 (C^{A6}), 129.6 (C^{E5}), 126.3 (C^{B5}), 125.9 (C^{E3}), 125.5 (C^{A4}), 125.4 (C^{A3}), 122.5 (C^{B3}), 60.3 (C^{CtBu}), 23.5 (C^{tBu}). IR (solid, ν/cm^{-1}) 2979 (w), 1607 (w), 1575 (w), 1475 (m), 1448 (w), 1430 (w), 1373 (w), 1285 (m), 1193 (w), 1129 (s), 1082 (m), 836 (s), 806 (m), 781 (m), 764 (m), 730 (w), 710 (m), 672 (m), 658 (m), 648 (m), 585 (m), 569 (m), 556 (s), 492 (m). UV/Vis (MeCN, 0.99×10^{-5} mol dm^{-3}) λ/nm (ε/dm^3 mol^{-1} cm^{-1}) 257 (59 000), 295 sh (35 000), 391 (4700), 420 sh (3400 dm^3 mol^{-1} cm^{-1}). Emission (MeCN, 0.99×10^{-5} mol dm^{-3}, λ_{exc} = 262 nm) λ_{em}^{max} = 493, 523 nm. ESI-MS m/z 897.2 $[M - PF_6]^+$ (calc. 897.2). Found C 45.51, H 4.05, N 5.56; $C_{40}H_{40}F_6IrN_4O_4PS_2 \cdot H_2O$ requires C 45.32, H 3.99, N 5.29%.

$[Ir(\mathbf{6})_2(bpy)][PF_6]$. 1-Dodecanethiol (0.060 mL, 50.4 mg, 0.249 mmol) was added to a suspension of NaH (60% in mineral oil, 10.0 mg, 0.250 mmol) in DMF (2 mL) under N_2. The mixture was stirred at room temperature for 10 min. $[Ir(\mathbf{1})_2(bpy)][PF_6]$ (53.0 mg, 0.0633 mmol) was added to the reaction mixture; this was heated at 120 °C for 1.5 h. The dark brown mixture was allowed to cool to room temperature and was then poured into a mixture of H_2O and brine (3 : 1 by vol.,

20 mL). The resulting suspension was stirred for 30 min at room temperature. The brown-yellow precipitate was separated by filtration and was washed with H_2O. The solid was redissolved in CH_2Cl_2 and the solution dried over Na_2SO_4. Solvent was removed *in vacuo* and the product was purified by column chromatography (silica, CH_2Cl_2 changing to CH_2Cl_2–2% MeOH). $[Ir(\mathbf{6})_2(bpy)][PF_6]$ was isolated as an orange solid (56.1 mg, 0.0467 mmol, 73.8%). ^{1}H NMR (500 MHz, CD_3CN) δ/ppm 8.54 (*pseudo*-dt, J = 8.3, 1.0 Hz, 2H, H^{E3}), 8.15 (*pseudo*-td, J = 7.9, 1.6 Hz, 2H, H^{E4}), 8.06 (m, 2H, H^{E6}), 8.00 (*pseudo*-dt, J = 8.4, 1.1 Hz, 2H, H^{B3}), 7.83 (m, 2H, H^{B4}), 7.68 (d, J = 8.3 Hz, 2H, H^{A3}), 7.58 (*pseudo*-dt, J = 5.9, 1.1 Hz, 2H, H^{B6}), 7.53 (ddd, J = 7.7, 5.4, 1.2 Hz, 2H, H^{E5}), 7.00 (ddd, J = 7.3, 5.8, 1.4 Hz, 2H, H^{B5}), 6.94 (dd, J = 8.2, 1.9 Hz, 2H, H^{A4}), 6.09 (d, J = 1.9 Hz, 2H, H^{A6}), 2.63 (m, 4H, H^{SCH2}), 1.40 (m, 4H, $H^{SCH2CH2}$), 1.35–1.16 (m, 36H, H^{CH2}), 0.89 (t, J = 7.0 Hz, 6H, H^{CH3}). $^{13}C\{^1H\}$ NMR (126 MHz, CD_3CN) δ/ppm 168.0 (C^{B2}), 156.7 (C^{E2}), 151.8 (C^{A1+E6}), 150.1 (C^{B6}), 141.6 (C^{A2}), 141.5 (C^{A5}), 140.3 (C^{E4}), 139.4 (C^{B4}), 129.4 (C^{E5}), 128.7 (C^{A6}), 126.1 (C^{A3}), 125.6 (C^{E3}), 123.9 (C^{B5}), 122.0 (C^{A4}), 120.5 (C^{B3}), 32.6 (C^{CH2}), 32.0 (C^{SCH2}), 30.3 ($2C^{CH2}$), 30.25 (C^{CH2}), 30.2 (C^{CH2}), 30.1 (C^{CH2}), 29.9 (C^{CH2}), 29.7 ($C^{SCH2CH2}$), 29.4 (C^{CH2}), 23.4 (C^{CH2}), 14.4 (S^{CH3}). IR (solid, ν/cm^{-1}) 2922 (m), 2852 (m), 1606 (m), 1567 (m), 1537 (w), 1472 (m), 1446 (m), 1423 (m), 1373 (w), 1315 (w), 1261 (w), 1244 (w), 1164 (w), 1095 (m), 1062 (w), 1030 (w), 876 (w), 835 (s), 791 (m), 769 (s), 732 (m), 650 (w), 639 (w), 556 (s), 520 (w). UV/Vis (MeCN, 0.99 × 10^{-5} mol dm^{-3}) λ/nm (ε/dm^3 mol^{-1} cm^{-1}) 251 (41 000), 310 (36 000), 400 sh (8200). Emission (MeCN, 0.99 × 10^{-5} mol dm^{-3}, λ_{exc} = 252 nm) λ_{em}^{max} = 577 nm. ESI-MS m/z 1058.1 $[M - PF_6]^+$ calc. 1057.5. Found C 56.02, H 6.00, N 4.73; $C_{56}H_{72}F_6IrN_4PS_2$ requires C 55.93, H 6.04, N 4.66%.

$[Ir(\mathbf{7})_2(bpy)][PF_6]$. $[Ir_2(\mathbf{7})_4Cl_2]$ (214 mg, 0.107 mmol) and bpy (50.1 mg, 0.321 mmol) were suspended in MeOH (15 mL) and the mixture was heated at reflux for 2 d. After cooling to room temperature, the mixture was filtered. An excess of NH_4PF_6 followed by H_2O were added to the orange filtrate and the resulting suspension was stirred for 5 min. The precipitate was collected by filtration, was washed with H_2O and redissolved in CH_2Cl_2. Solvent was removed *in vacuo* and the residue was purified twice by column chromatography (silica, CH_2Cl_2 changing to CH_2Cl_2–1% MeOH; silica, CH_2Cl_2–1% MeOH). $[Ir(\mathbf{7})_2(bpy)][PF_6]$ was isolated as a yellow solid (81.1 mg, 0.0640 mmol, 30.0%). ^{1}H NMR (500 MHz, CD_3CN) δ/ppm 8.56 (*pseudo*-dt, J = 8.4, 1.0 Hz, 2H, H^{E3}), 8.23 (*pseudo*-dt, J = 8.1, 0.9 Hz, 2H, H^{B3}), 8.17 (*pseudo*-td, J = 7.9, 1.5 Hz, 2H, H^{E4}), 8.04–7.96 (overlapping m, 6H, $H^{A3+B4+E6}$), 7.71 (m, 2H, H^{B6}), 7.50 (m, 4H, H^{A4+E5}), 7.21 (ddd, J = 7.5, 5.8, 1.4 Hz, 2H, H^{B5}), 6.58 (d, J = 1.8 Hz, 2H, H^{A6}), 2.87 (m, 4H, H^{SO2CH2}), 1.40–1.01 (overlapping m, 40H, H^{CH2}), 0.88 (t, J = 7.1 Hz, 6H, H^{CH3}). $^{13}C\{^1H\}$ NMR (126 MHz, CD_3CN) δ/ppm 166.2 (C^{B2}), 156.6 (C^{E2}), 152.1 (C^{E6}), 151.1 ($C^{A1/A5}$), 150.9 (C^{B6}), 150.1 (C^{A2}), 140.8 (C^{E4}), 140.4 (C^{B4}), 140.3 ($C^{A5/A1}$), 130.8 (C^{A6}), 129.6 (C^{E5}), 126.3 (C^{B5}), 126.2 (C^{A3}), 125.9 (C^{E3}), 123.2 (C^{A4}), 122.5 (C^{B3}), 56.3 (C^{SO2CH2}), 32.6 (C^{CH2}), 30.33 (C^{CH2}), 30.32 (C^{CH2}), 30.2 (C^{CH2}), 30.1 (C^{CH2}), 30.0 (C^{CH2}), 29.7 (C^{CH2}), 28.6 (C^{CH2}), 23.8 (C^{CH2}), 23.4 (C^{CH2}), 14.4 (C^{CH3}). IR (solid, ν/cm^{-1}) 2923 (m), 2853 (w), 1608 (w), 1576 (w), 1476 (m), 1448 (w), 1430 (w), 1375 (w), 1294 (m), 1140 (s), 1090 (m), 1063 (w), 836 (s), 762 (s), 728 (m), 667 (m), 652 (w), 606 (m), 582 (w), 556 (s), 500 (m). UV/Vis (MeCN, 1.0 × 10^{-5} mol dm^{-3}) λ/nm (ε/dm^3 mol^{-1} cm^{-1}) 256 (58 000), 310 sh (25 000), 350 sh (7900), 390 (5000), 420 sh (3700 dm^3 mol^{-1} cm^{-1}). Emission (MeCN, 1.0 × 10^{-5} mol dm^{-3}, λ_{exc} = 262 nm) λ_{em}^{max} = 493, 524 nm. ESI-MS m/z 1121.6 $[M - PF_6]^+$ (calc. 1121.5). Found C 53.38, H 5.57, N 4.72; $C_{56}H_{72}F_6IrN_4O_4PS_2$ requires C 53.11, H 5.73, N 4.42%.

Crystallography

Data were collected on a Bruker-Nonius KappaAPEX diffractometer with data reduction, solution and refinement using the programs APEX2[24] and SHELXL97.[25] ORTEP-type diagrams and structure analysis used Mercury v. 3.0.[26,27] Crystallographic data are given in Table 1.

Results and discussion

Ligand synthesis and characterization

The fluoro compound H**1** is a convenient precursor to each of H**2**, H**4** and H**6**. The thiomethyl group in H**2** is readily introduced by treatment of H**1** with NaSMe in NMP under microwave conditions. The 93% yield of H**2** is superior to the 10% obtained using the reported Ullmann coupling of 2-bromopyridine and 4-bromothianisole.[23] The synthesis of H**4** was adapted from that reported for the formation of 2(2-^{t}butylthiophenyl)pyridine,[28] and H**6** was prepared in a similar manner. For each, the appropriate thiol was treated with NaH in DMF to generate the corresponding thiolate to displace the fluoro group from H**1**. Of the oxidation strategies tried for conversion of the thiols to corresponding sulfones, use of Na_2WO_4–H_2O_2[29] proved to be the most efficient.

Compounds H**2**–H**8** were characterized by routine spectroscopic methods, mass spectrometry and elemental analysis. The base peak in the electrospray mass spectrum of H**2**, H**3**, H**4**, H**5** and H**7** corresponded to the $[M + H]^+$ with the isotopic distribution matching that calculated in each case. For H**6**, a parent ion (m/z 355.7) was observed in the MALDI-TOF mass spectrum, but no $[M + H]^+$ ion was detected in the ESI-MS. ^{1}H and ^{13}C NMR spectra were assigned using 2D methods (COSY, HMQC and HMBC) and were consistent with the structures shown in Scheme 1.

Single crystals of H**3** were grown by overlaying a $CHCl_3$ solution with hexanes, and of H**5** by overlaying a CH_2Cl_2 solution with hexanes. The structures are shown in Fig. 1 and 2. Both compounds crystallize in the monoclinic space group $C2/c$. Detailed analyses of the structures of a range of aryl–alkyl sulfones[30] and diaryl sulfones[30,31] illustrate the formation both intra- and intermolecular $CH_{aryl}\cdots OS$ hydrogen bonds. In H**3**, the O1–S1–C9–C10 and O2–S1–C9–C8 torsion angles are −25.0(1) and 28.2(1)°, respectively, leading to intramolecular O1···H10a and O2···H8a contacts of 2.60 and 2.64 Å. In H**5**, the corresponding angles (O1–S1–C9–C8 and O2–S1–C9–C10)

Table 1 Crystallographic data

Compound	H3	H5	$[Ir_2(3)_4Cl_2]\cdot 2CH_2Cl_2$	Δ-$[Ir(1)_2(bpy)][PF_6]$	*rac*-4{$[Ir(1)_2(bpy)][PF_6]$}·$Et_2O\cdot 2CH_2Cl_2$
Formula	$C_{12}H_{11}NO_2S$	$C_{15}H_{17}NO_2S$	$C_{50}H_{44}Cl_6Ir_2N_4O_8S_4$	$C_{32}H_{22}F_2IrN_4P$	$C_{134}H_{102}Cl_4F_{32}Ir_4N_{16}OP_4$
Formula weight	233.29	275.37	1554.31	837.73	3594.88
Crystal colour and habit	Colourless block	Colourless block	Yellow plate	Yellow block	Yellow block
Crystal system	Monoclinic	Monoclinic	Orthorhombic	Trigonal	Triclinic
Space group	*C*2/*c*	*C*2/*c*	*Pbca*	$P3_121$	$P\bar{1}$
a, *b*, *c*/Å	23.4437(15)	22.2664(12)	22.0732(12)	13.9523(9)	14.2353(6)
	7.1763(5)	6.1121(4)	21.3598(11)	13.9523(9)	16.2890(7)
	16.5008(11)	22.0876(11)	23.0604(12)	26.0654(17)	17.6451(7)
α, *β*, *γ*/°	90	90	90	90	66.1650(10)
	129.026(3)	110.398(2)	90	90	81.642(2)
	90	90	90	120	67.3900(10)
U/ Å^3	2156.6(2)	2817.5(3)	10 872.5(10)	4394.3(6)	3454.7(3)
Dc/Mg m^{-3}	1.437	1.298	1.899	1.899	1.728
Z	8	8	8	6	1
μ(M-Kα)/mm^{-1}	0.282 (M = Mo)	2.019 (M = Mo)	13.963 (M = Cu)	10.083 (M = Cu)	9.298 (M = Cu)
T/K	123	296	123	123	296
Refln. collected (R_{int})	30 251 (0.0269)	7450 (0.0275)	59 052 (0.1107)	67 974 (0.0341)	23 674 (0.0287)
Unique refln.	3021	2523	9726	5359	11 699
Refln. for refinement	2681	2228	6764	5311	10 552
Parameters	146	175	699	415	906
Threshold	$I > 2.0\sigma$	$I > 2.0\sigma$	$I > 2.0\sigma$	$I > 2.0\sigma$	$I > 2.0\sigma$
R_1 (R_1 all data)	0.0323 (0.0376)	0.0378 (0.0420)	0.0470 (0.0820)	0.0170 (0.0172)	0.0368 (0.0399)
wR_2 (wR_2 all data)	0.0913 (0.0962)	0.1024 (0.1068)	0.1111 (0.1295)	0.0436 (0.0437)	0.1120 (0.1168)
Goodness of fit	1.057	1.080	1.008	1.098	1.036
Flack parameter	—	—	—	0.007(2)	—
CCDC deposition	972690	972692	972691	972693	972694

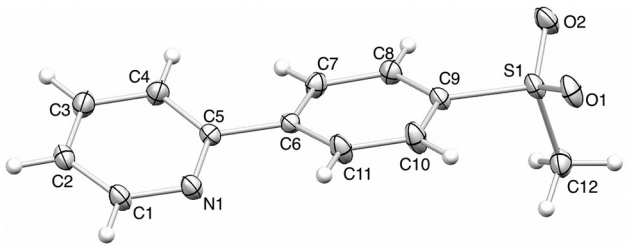

Fig. 1 ORTEP representation of the structure of H3 (ellipsoids plotted at 40% probability level). Selected bond lengths and angles: S1–O2 = 1.4411(9), S1–O1 = 1.4434(10), S1–C12 = 1.7569(14), S1–C9 = 1.7575(11) Å; O2–S1–O1 = 118.19(6), O2–S1–C12 = 108.03(7), O1–S1–C12 = 108.11(6), O2–S1–C9 = 109.20(6), O1–S1–C9 = 108.45(6), C12–S1–C9 = 103.93(6)°.

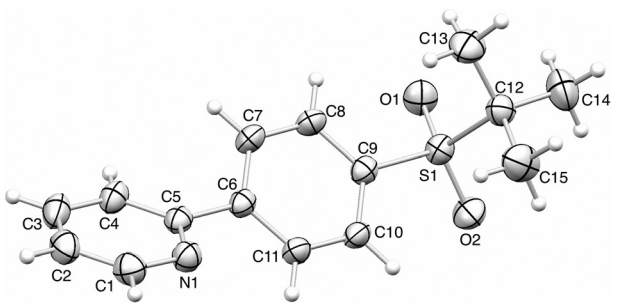

Fig. 2 ORTEP representation of the structure of H5 (ellipsoids plotted at 40% probability level). Selected bond distances and angles: S1–O2 = 1.4378(12), S1–O1 = 1.4402(12), S1–C12 = 1.8190(16), S1–C9 = 1.7727(15) Å; O2–S1–O1 = 118.85(8), O2–S1–C9 = 107.48(7), O1–S1–C9 = 107.03(7), O2–S1–C12 = 108.05(8), O1–S1–C12 = 107.50(8), C9–S1–C12 = 107.46(7)°.

are −23.1(1) and 24.6(1)° with O1···H8a and O2···H10a separations of 2.57 and 2.64 Å. The dihedral angles between the phenyl and pyridine rings are 17.7° in H3, and 37.7° in H5. This marked difference is associated with face-to-face π-stacking of phenyl and pyridine rings in H3 (but not in H5). Centrosymmetric pairs of H3 molecules interact through a slipped arrangement of aromatic rings (Fig. 3a) with an intercentroid distance of 3.81 Å. The sulfone group engages in hydrogen-bonded contacts to the methyl groups of two adjacent molecules and the pyridine ring CH of a third molecule. In contrast, a primary packing interaction in H5 involves $CH_{phenyl}\cdots O_{sulfone}$ contacts resulting in the formation of ribbons of hydrogen-bonded molecules (Fig. 3b). The ^{t}butyl groups protrude along one side of the ribbon, and pairs of adjacent ribbons associate through short $CH_{butyl}\cdots N_{pyridine}$ contacts (2.73 Å) giving an extended domain of ^{t}butyl units sandwiched between aromatic domains (Fig. 3c).

Synthesis and characterization of $[Ir_2(C\hat{}N)_4Cl_2]$ dimers

Complexes in the $[Ir(ppy)_2(N\hat{}N)]^+$ family are usually synthesized by reaction between the N^N ligand and the chlorido-bridged dimer $[Ir_2(ppy)_4Cl_2]$.[32] Typically, this dimer is prepared from the reaction of $IrCl_3\cdot nH_2O$ with Hppy.[33,34] Although $[Ir_2(1)_4Cl_2]$ (prepared by the latter method) has previously been described,[6] the remaining chlorido-bridged precursors to the target complexes $[Ir(C\hat{}N)_2(bpy)]^+$ with C^N = 2 to 7 have not, to the best of our knowledge, been previously reported.

The reaction of $IrCl_3\cdot nH_2O$ with sulfones H5 and H7 proceeded smoothly under reflux in a mixture of 2-ethoxyethanol and water (Scheme 2). The compounds $[Ir_2(5)_4Cl_2]$ and

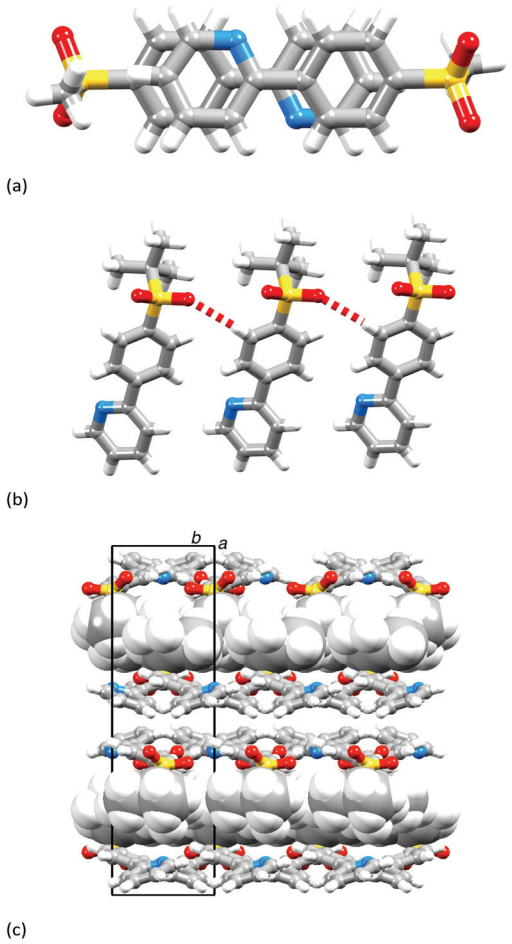

Fig. 3 (a) Face-to-face interactions between centrosymmetric pairs of molecules of H**3**. (b) Ribbon formation through $CH_{phenyl}\cdots O_{sulfone}$ contacts in H**5**. (c) Sandwiching of ^{t}butyl (space-filling) units between aromatic domains in H**5**.

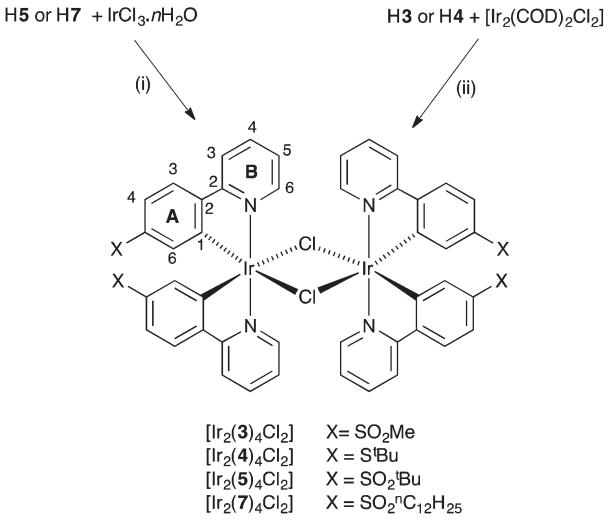

Scheme 2 Routes to the dimers $[Ir_2(C\hat{}N)_4Cl_2]$ with C^N = **3**, **4**, **5** and **7**. Conditions: (i) 2-ethoxyethanol–H_2O, reflux ≈22 h; (ii) 2-ethoxyethanol; reflux overnight (for H**3**), or 110 °C, 1.5 h under microwave conditions (for H**4**).

$[Ir_2(\mathbf{7})_4Cl_2]$ were isolated as yellow solids. The ^{1}H and ^{13}C NMR spectra of the complexes showed negligible impurities and the compounds were used in the next step (see the next section) without purification. The NMR spectra were assigned using routine 2D methods and were in accord with the structures shown in Scheme 2. For a MeOH solution of $[Ir_2(\mathbf{5})_4Cl_2]$, the second most intense peak in the electrospray mass spectrum came at *m*/*z* 741.2 and as assigned to the $[Ir(\mathbf{5})_2]^+$ ion. The base peak at *m*/*z* 782.1 and a lower intensity peak at *m*/*z* 823.1 arose from $[Ir(\mathbf{5})_2(MeCN)]^+$ and $[Ir(\mathbf{5})_2(MeCN)_2]^+$, respectively; we assume that the MeCN arises from the eluent in the LC column of the LC-ESI-MS. The isotope distributions for each peak matched the calculated patterns. MALDI-TOF mass spectrometry proved more amenable to observing a mass spectrum of $[Ir_2(\mathbf{7})_4Cl_2]$, with the base peak at *m*/*z* 965.9 corresponding to $[Ir(\mathbf{7})_2]^+$.

Attempts to prepare the dimers $[Ir_2(C\hat{}N)_4Cl_2]$ with C^N = **2**, **3** or **4** from reactions of H**2**, H**3** or H**4** with $IrCl_3{\cdot}nH_2O$ were unsuccessful. We therefore adopted an alternative strategy which involves the reaction of the conjugate acid of the cyclometalling ligand with $[Ir_2(COD)_2Cl_2]$.[35] Unfortunately, reaction of H**2** with $[Ir_2(COD)_2Cl_2]$ gave an insoluble solid which could not be characterized, and attempts to prepare and isolate $[Ir_2(\mathbf{2})_4Cl_2]$ were abandoned. We note that the latter insoluble material reacted with bpy in MeOH to give a mixture of products rather than a salt of the desired $[Ir(\mathbf{2})_2(bpy)]^+$.

The reaction of $[Ir_2(COD)_2Cl_2]$ with H**3** and H**4** (Scheme 2) yielded $[Ir_2(\mathbf{3})_4Cl_2]$ and $[Ir_2(\mathbf{4})_4Cl_2]$ as yellow powders in good yields. As judged by ^{1}H NMR spectroscopy, the crude products were pure enough to be used directly in the next step (see the next section). The solution ^{1}H and ^{13}C NMR spectra of $[Ir_2(\mathbf{3})_4Cl_2]$ were assigned by COSY, HMQC and HMBC methods and were in accord with the structures in Scheme 2. In contrast, $[Ir_2(\mathbf{4})_4Cl_2]$ is poorly soluble in most common organic solvents. The ^{1}H NMR spectrum was assigned using a COSY spectrum and by comparison with those of the other dimers, but the 1D ^{13}C NMR spectrum and the 2D HMQC and HMBC spectra were too poorly resolved to permit ^{13}C NMR data to be determined. The electrospray mass spectrum of an MeOH solution of $[Ir_2(\mathbf{3})_4Cl_2]$ showed peaks at *m*/*z* 657.1 and 698.2 assigned to $[Ir(\mathbf{3})_2]^+$ and $[Ir(\mathbf{3})_2(MeCN)]^+$, respectively; (the origin of the MeCN is explained above). Analogous peaks were observed in the ESI mass spectrum of $[Ir_2(\mathbf{4})_4Cl_2]$.

The synthesis of $[Ir_2(\mathbf{6})_4Cl_2]$ could not be achieved by the reaction of $[Ir_2(COD)_2Cl_2]$ with H**6**, and unreacted ligand was recovered from the reaction mixture after 22 hours reflux in 2-ethoxyethanol.

Despite the widespread synthetic use of $[Ir_2(C\hat{}N)_4Cl_2]$ dimers, X-ray diffraction data for this family of complexes in which C^N is (or is derived from) a 2-phenylpyridine ligand remains sparse. A search of the Cambridge Structural Database[36] (CSD, v. 5.34 with November 2012, and February and May 2103 updates) using Conquest v. 1.35[26] generated only nine hits,[37–44] including the structures of the enantiomerically pure Λ,Λ- and Δ,Δ-forms[42] of $[Ir_2(ppy)_4Cl_2]$ as well as that of the centrosymmetric Δ,Λ-form.[41] In addition, we have recently

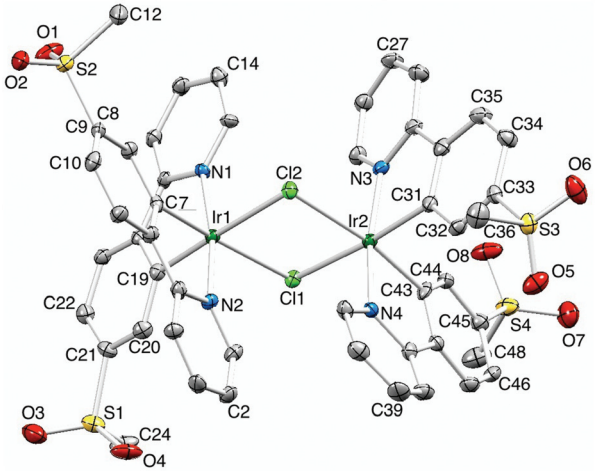

Fig. 4 ORTEP representation of $[Ir_2(\mathbf{3})_4Cl_2]$ in $[Ir_2(\mathbf{3})_4Cl_2]\cdot 2CH_2Cl_2$ (ellipsoids plotted at 30% probability level and H atoms omitted). Important bond parameters: Ir1–C19 = 1.984(8), Ir1–C7 = 1.988(8), Ir1–N1 = 2.050(7), Ir1–N2 = 2.057(7), Ir1–Cl1 = 2.486(2), Ir1–Cl2 = 2.512(2), Ir2–C43 = 1.995(8), Ir2–C31 = 2.015(9), Ir2–N4 = 2.043(7), Ir2–N3 = 2.053(7), Ir2–Cl2 = 2.503(2), Ir2–Cl1 = 2.504(2), S1–O3 = 1.404(9), S1–O4 = 1.441(8), S1–C21 = 1.778(9), S1–C24 = 1.786(10), O1–S2 = 1.422(8), O2–S2 = 1.439(7) Å; Cl1–Ir1–Cl2 = 84.46(7), Cl2–Ir2–Cl1 = 84.30(6), C19–Ir1–N1 = 80.2(3), C7–Ir1–N2 = 80.9(3), C31–Ir2–N3 = 80.7(3), O3–S1–O4 = 117.5(5), O1–S2–O2 = 117.0(5), O6–S3–O5 = 119.7(5), O7–S4–O8 = 117.1(6)°.

reported the structure of $[Ir_2(dfppz)_2(\mu\text{-}Cl)_2]\cdot CH_2Cl_2$ (Hdfppz = 1-(2,4-difluorophenyl)-1*H*-pyrazole).[45] Single crystals of $[Ir_2(\mathbf{3})_4Cl_2]\cdot 2CH_2Cl_2$ were grown from a CH_2Cl_2 solution of the complex overlaid with Et_2O. The structure of the dimer is shown in Fig. 4; each iridium atom is in an octahedral environment. The complex crystallizes in the orthorhombic space group *Pbca* and the asymmetric unit contains the Λ,Λ-enantiomer with both the Λ,Λ- and Δ,Δ-forms present in the lattice. As in other $[Ir_2(C\text{^}N)_4Cl_2]$ dimers and in mononuclear $[Ir(C\text{^}N)_2(N\text{^}N)]^+$ cations, the two cyclometallated ligands are arranged with the N-donors *trans* to one another at each iridium centre. Bond parameters (cation to Fig. 4) are unexceptional. The orientations of the four independent sulfone groups with respect to the phenyl ring to which each is attached fall into two categories. Two are twisted in a similar manner to that in the free ligand H**3** (see above) with torsion angles of O1–S2–C9–C8 and O2–S2–C9–C10 = 30.9(9) and −20.5(9)° and O5–S3–C33–C32 and O6–S3–C33–C34 = 31.4(9) and −17.4(9)°. This arrangement gives rise to short $CH_{phenyl}\cdots O_{sulfone}$ contacts of 2.59 and 2.66 Å, and 2.56 and 2.62 Å, respectively (two per sulfone group). In contrast, the sulfone groups containing S1 and S4 are oriented such that the torsion angles are O3–S1–C21–C22 and O4–S1–C21–C20 = −58.2(9) and −3.3(9), and O7–S4–C45–C46 and O8–S4–C45–C44 = −53.8(9) and −1.3(9)°. This leads to one $CH_{phenyl}\cdots O_{sulfone}$ contact being more effective than the other (separations of 2.49 *versus* 2.99 Å, and 2.47 *versus* 2.96 Å). The CH_2Cl_2 solvate molecules sit in pockets between pairs of cyclometallated ligands bound to different iridium centres of the dimer. One CH_2Cl_2 molecule is disordered and has been modelled over two sites of fractional occupancies 0.62 and 0.38.

Synthesis and characterization of $[Ir(C\text{^}N)_2(bpy)][PF_6]$ complexes

Synthesis of the $[Ir(C\text{^}N)_2(bpy)][PF_6]$ complexes was initially approached using the established methodology[32] of treating the appropriate $[Ir_2(C\text{^}N)_4Cl_2]$ dimer with two equivalents of bpy. This method was successful in five out of six cases (Scheme 3a). $[Ir(\mathbf{1})_2(bpy)][PF_6]$, $[Ir(\mathbf{3})_2(bpy)][PF_6]$, $[Ir(\mathbf{4})_2(bpy)][PF_6]$ and $[Ir(\mathbf{5})_2(bpy)][PF_6]$ were isolated in yields ranging from 70.3 to 87.7%. Purification of $[Ir(\mathbf{4})_2(bpy)][PF_6]$ required a series of chromatographic and precipitation steps (see Experimental section), but a high yield was still obtained. Purification of $[Ir(\mathbf{7})_2(bpy)][PF_6]$ also required two chromatography columns and the final yield was only 30.0%; unreacted dimer was not recovered and the side products were not identified. Since the dimer $[Ir_2(\mathbf{6})_4Cl_2]$ could not be prepared (see above), we adopted a nucleophilic substitution approach to prepare $[Ir(\mathbf{6})_2(bpy)][PF_6]$ from $[Ir(\mathbf{1})_2(bpy)][PF_6]$ (Scheme 3b). The fluoro-derivative was treated with 1-dodecanethiol in the presence of sodium hydride and, after workup, $[Ir(\mathbf{6})_2(bpy)][PF_6]$ was obtained in 73.8% yield. We have recently demonstrated that the presence of small amounts of chloride ion can have significant negative impact on the performance of materials in LECs, and all new compounds were shown to exhibit no changes in their ^1H NMR spectra upon the addition of $[^nBu_4N][PF_6]$.[46]

The base peak in the electrospray mass spectrum of each $[Ir(C\text{^}N)_2(bpy)][PF_6]$ complex consisted of a peak envelope corresponding to $[M - PF_6]^+$ exhibiting the characteristic isotopic distribution for iridium. The ^1H and ^{13}C NMR spectra of each complex were consistent with a C_2-symmetric cation. Fig. 5 shows the ^1H NMR spectrum of $[Ir(\mathbf{5})_2(bpy)][PF_6]$ as a representative example. Signals in the ^1H and ^{13}C NMR spectra were assigned using a combination of COSY, HMQC and HMBC methods. The ^1H NMR signal for the ^{t}butyl group in $[Ir(\mathbf{4})_2(bpy)][PF_6]$ appears at δ 1.00 ppm and shifts to lower frequency (δ 0.93 ppm) in the analogous sulfone derivative $[Ir(\mathbf{5})_2(bpy)][PF_6]$. The ^{13}C NMR resonance for the primary carbon atom in the ^{t}butyl group shifts from δ 31.1 to 23.5 ppm on going from $[Ir(\mathbf{4})_2(bpy)][PF_6]$ to $[Ir(\mathbf{5})_2(bpy)][PF_6]$, while the S-attached ^{13}C nucleus resonates at δ 46.8 and 60.3 ppm, respectively, in the sulfane and sulfone complexes. In $[Ir(\mathbf{6})_2(bpy)][PF_6]$ and $[Ir(\mathbf{7})_2(bpy)][PF_6]$, the SCH_2 unit is characterized by signals at $\delta(^1H)$ 2.63 ppm and $\delta(^{13}C)$ 32.0 ppm in the sulfane and $\delta(^1H)$ 2.87 ppm and $\delta(^{13}C)$ 56.3 ppm in the sulfone. Across the series of $[Ir(C\text{^}N)_2(bpy)][PF_6]$ complexes, the only bpy-proton signal to be noticeably affected is that assigned to H^{E6} (see Scheme 3) since only this bpy proton is directed towards the substituted phenyl ring. As expected, signals arising from the phenyl-ring protons (H^{A3}, H^{A4} and H^{A6}) undergo the most significant changes in chemical shift. For each pair of sulfane and sulfone complexes, signals for H^{A3}, H^{A4} and H^{A6} all move to higher frequency ($\Delta\delta$ is in the range 0.20 and 0.56 ppm). Signals for protons H^{A6} and H^{A4}

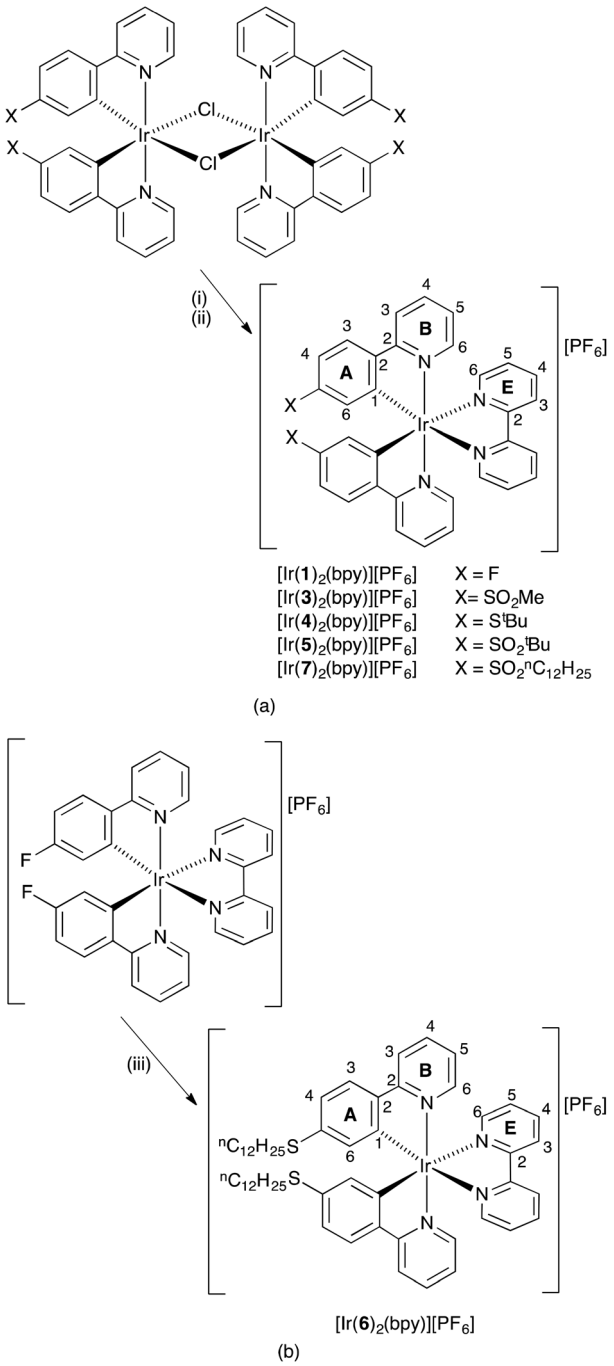

Scheme 3 Synthetic routes to the $[Ir(C\hat{}N)_2(N\hat{}N)][PF_6]$ complexes. In route (a), conditions: (i) bpy, MeOH at reflux or in microwave reactor, 120 °C; (ii) NH_4PF_6. In route (b), conditions: (iii) $^nC_{12}H_{25}SH$, NaH, DMF, 120 °C. Atom labelling for NMR spectroscopic assignments is shown.

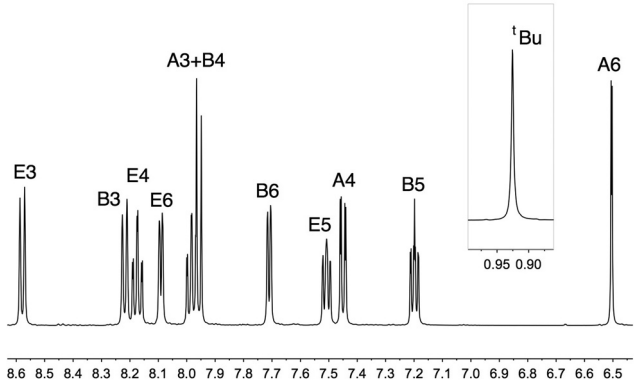

Fig. 5 500 MHz ^1H NMR spectrum (295 K, CD_3CN) of $[Ir(\mathbf{5})_2(bpy)][PF_6]$; see Scheme 3 for proton labelling. Scale: δ /ppm.

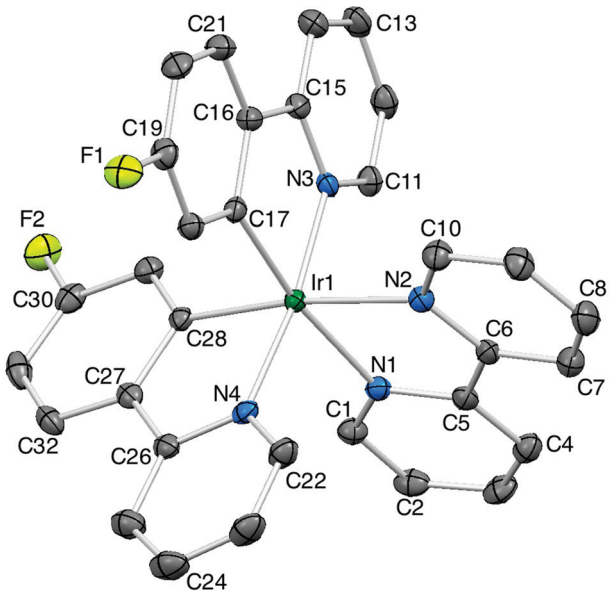

Fig. 6 ORTEP representation of the Δ-$[Ir(\mathbf{1})_2(bpy)]^+$ in Δ-$[Ir(\mathbf{1})_2(bpy)][PF_6]$ (ellipsoids plotted at 40% probability level and H atoms omitted). Selected bond parameters: Ir1–C17 = 2.008(4), Ir1–C28 = 2.008(4), Ir1–N3 = 2.048(3), Ir1–N4 = 2.054(3), Ir1–N1 = 2.130(3), Ir1–N2 = 2.141(3), C19–F1 = 1.374(5), C30–F2 = 1.370(5) Å; N1–Ir1–N2 = 76.95(12), C17–Ir1–N3 = 80.17(14), C28–Ir1–N4 = 80.77(14), N3–Ir1–N4 = 172.38(12), C17–Ir1–N1 = 170.94(13), C28–Ir1–N2 = 172.58(13)°.

undergo the largest shifts to lower frequency in the fluoro-derivative, appearing at δ 5.89 and 6.81 ppm, respectively.

Single-crystal data were collected for $[Ir(\mathbf{1})_2(bpy)][PF_6]$ (crystals being grown from MeCN or CH_2Cl_2 solutions of the complex overlaid with Et_2O, respectively) and fortuitously resulted in the determination of the structures of Δ-$[Ir(\mathbf{1})_2(bpy)][PF_6]$ and *rac*-4{$[Ir(\mathbf{1})_2(bpy)][PF_6]$}·$Et_2O$·$2CH_2Cl_2$. Enantiomerically pure Δ-$[Ir(\mathbf{1})_2(bpy)][PF_6]$ crystallizes in the trigonal space group $P3_121$ and Fig. 6 shows the structure of the Δ-$[Ir(\mathbf{1})_2(bpy)]^+$ cation. The octahedral environment of Ir1 with *trans*-arrangement of the N donors (N3 and N4) of the cyclometallating ligands is as expected, and bond parameters (see Fig. 6 caption) are typical. We note that the packing interactions are predominantly CH···F contacts involving the F atoms of both the $[PF_6]^-$ anions and the fluorophenyl rings. There are no π-stacking interactions between arene rings of adjacent cations. This is in contrast to those observed in *rac*-$[Ir(\mathbf{1})_2(bpy)][PF_6]$ described below.

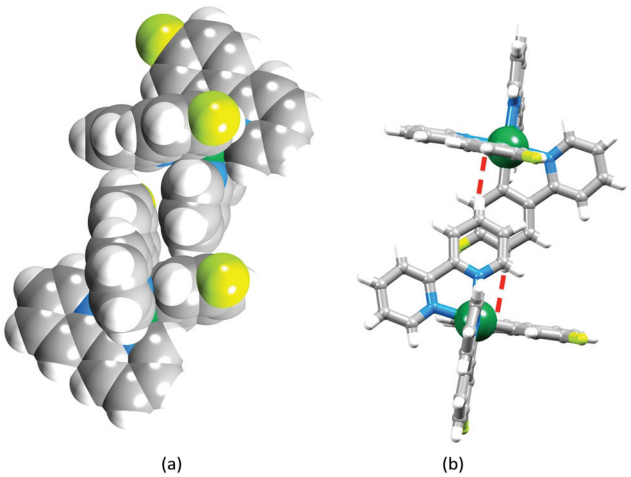

Fig. 7 Face-to-face/edge-to-face embrace between the two independent Δ and Λ-$[Ir(\mathbf{1})_2(bpy)]^+$ cations in *rac*-4{$[Ir(\mathbf{1})_2(bpy)][PF_6]$}·$Et_2O{\cdot}2CH_2Cl_2$: (a) space-filling, and (b) showing relative orientations of the fluorophenyl and pyridine rings involved in the face-to-face interaction and CH···π contacts (red hashed lines).

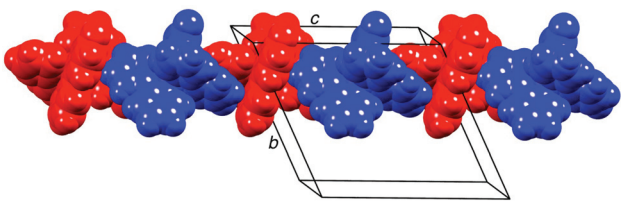

Fig. 8 Chain of alternating Δ- (red) and Λ- (blue) $[Ir(\mathbf{1})_2(bpy)]^+$ cations in *rac*-4{$[Ir(\mathbf{1})_2(bpy)][PF_6]$}·$Et_2O{\cdot}2CH_2Cl_2$.

The racemate crystallizes as the solvate *rac*-4{$[Ir(\mathbf{1})_2(bpy)][PF_6]$}·$Et_2O{\cdot}2CH_2Cl_2$ in the triclinic space group $P\bar{1}$. In terms of bond parameters, the structure of each enantiomer of the $[Ir(\mathbf{1})_2(bpy)]^+$ cation is similar to that of the Δ-$[Ir(\mathbf{1})_2(bpy)]^+$ cation described above and we focus only upon the packing interactions. The asymmetric unit in 4{$[Ir(\mathbf{1})_2(bpy)][PF_6]$}·$Et_2O{\cdot}2CH_2Cl_2$ contains two $[Ir(\mathbf{1})_2(bpy)]^+$ cations of opposite handedness which engage in an embrace[47] involving face-to-face and edge-to-face π-interactions (Fig. 7). The face-to-face contact is between a fluorophenyl ring and one pyridine ring of a bpy ligand; the rings are slipped such that the F atom lies partly over the pyridine π-system[48,49] (Fig. 7b) and the interplane angle is 12.4°. The centroid···centroid separation of 4.24 Å lies towards the upper end of the typical range of interactions involving pyridine rings.[50] For the CH···π contacts (one $CH_{fluoroPh}\cdots\pi_{py}$ and one $CH_{py}\cdots\pi_{fluoroPh}$), the CH···centroid distances are 2.59 and 3.03 Å. Face-to-face π-interactions between crystallographically independent Δ- and Λ-$[Ir(\mathbf{1})_2(bpy)]^+$ cations extend beyond the single pair in the asymmetric unit to generate chains that run parallel to the *c*-axis (Fig. 8). The $[PF_6]^-$ anions are ordered; atoms P2 and P3 reside on inversion centres with half of each respective anion present in the asymmetric unit. Extensive CH···F contacts contribute to the crystal packing. The CH_2Cl_2 solvent molecule is ordered, and the Et_2O molecule is half occupancy.

Photophysical properties

The solution electronic absorption spectra of $[Ir(C\hat{}N)_2(bpy)][PF_6]$ (C^N = **1**, **3**–**7**) are shown in Fig. 9. All are dominated by intense high-energy bands which we assign to ligand-centred (LC), spin-allowed π*←π or π*←n transitions. The origin of the lower intensity and broader spectrum of $[Ir(\mathbf{6})_2(bpy)][PF_6]$ is not readily interpreted, but reproducibility with different batches of compound was confirmed. All spectra extend into the visible region, consistent with the yellow colour of the compounds $[Ir(C\hat{}N)_2(bpy)][PF_6]$ (C^N = **1**, **3**–**5**, **7**) and orange colour of $[Ir(\mathbf{6})_2(bpy)][PF_6]$. Absorptions at wavelengths in the approximate range 350 to 450 nm are attributed to low intensity ^{1}MLCT and ^{1}LLCT bands.[1]

Excitation of MeCN solutions of the complexes with λ_{exc} varying between 269 and 300 for $[Ir(\mathbf{1})_2(bpy)][PF_6]$, and between 252 and 400 nm for the other complexes results in the emission spectra shown in Fig. 10. The spectra are invariant of chosen values of λ_{exc} in the above ranges with the exception of the appearance of the relevant harmonic band. The complexes $[Ir(\mathbf{1})_2(bpy)][PF_6]$, $[Ir(\mathbf{4})_2(bpy)][PF_6]$ and $[Ir(\mathbf{6})_2(bpy)][PF_6]$ (*i.e.* fluoro and sulfane substituents on the C^N ligands) are yellow emitters and the emission bands are broad and featureless. In contrast, $[Ir(\mathbf{3})_2(bpy)][PF_6]$, $[Ir(\mathbf{5})_2(bpy)][PF_6]$ and $[Ir(\mathbf{7})_2(bpy)][PF_6]$ are green emitters and the emission spectra exhibit vibrational structure. The emitting state of $[Ir(C\hat{}N)_2(N\hat{}N)]^+$ is the lowest energy triplet state which may contain contributions from ^{3}MLCT, ^{3}LC and ^{3}LLCT states.[1] Significant charge-transfer contributions lead to broad emission bands, but when the CT contributions are small, structured emissions are observed as is the case for the sulfone-containing complexes $[Ir(\mathbf{3})_2(bpy)][PF_6]$, $[Ir(\mathbf{5})_2(bpy)][PF_6]$ and $[Ir(\mathbf{7})_2(bpy)][PF_6]$. Table 2 summarizes the room temperature solution photophysical properties of the complexes. Compared

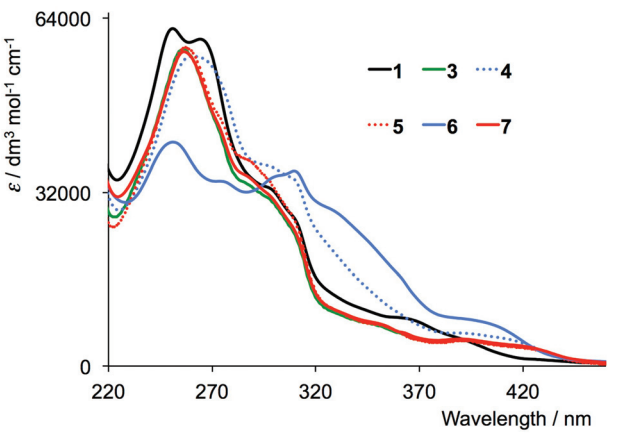

Fig. 9 Absorption spectra of MeCN solutions of $[Ir(C\hat{}N)_2(bpy)][PF_6]$ for C^N = **1**, **3**, **4**, **5**, **6** and **7**. See experimental section for concentrations.

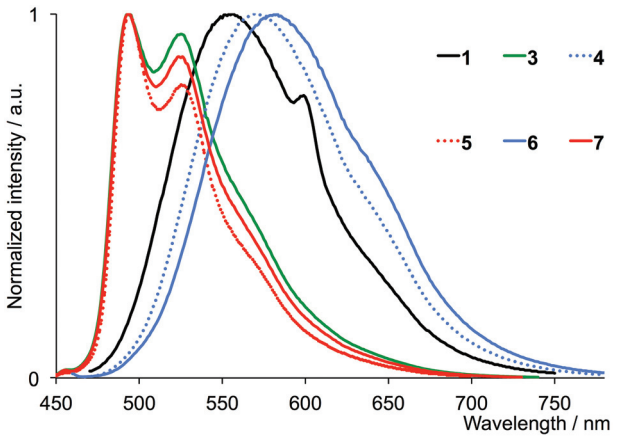

Fig. 10 Solution emission spectra of $[Ir(C\hat{}N)_2(bpy)][PF_6]$ for C^N = **1**, **3**, **4**, **5**, **6** and **7** (298 K, MeCN). See experimental section for solution concentrations. Excitation wavelengths: 300 nm (with **1**) and 400 nm (with **3**, **4**, **5**, **6** and **7**). * = Harmonic at 600 nm.

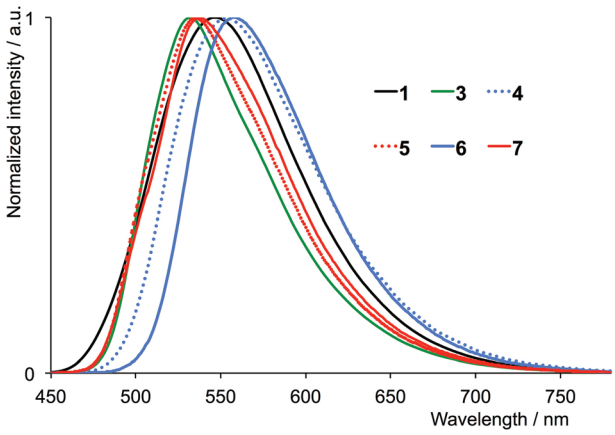

Fig. 11 Solid-state emission spectra of $[Ir(C\hat{}N)_2(bpy)][PF_6]$ for C^N = **1** and **3**–**7**. Excitation wavelengths: see Table 3.

Table 2 Solution photophysical properties of $[Ir(C\hat{}N)_2(bpy)][PF_6]$ (C^N = **1**, **3**–**7**). PLQY measured in de-aerated MeCN; lifetimes measured in de-aerated MeCN under argon atmosphere

Complex	λ_{exc}/nm	λ_{em}^{max}/nm	$\tau_{1/2}$ [a]/μs	PLQY/%
$[Ir(\mathbf{1})_2(bpy)][PF_6]$	269	557	0.224	36
$[Ir(\mathbf{3})_2(bpy)][PF_6]$	262	493, 525	2.33	74
$[Ir(\mathbf{4})_2(bpy)][PF_6]$	260	568	0.528	24
$[Ir(\mathbf{5})_2(bpy)][PF_6]$	262	493, 523	3.36	64
$[Ir(\mathbf{6})_2(bpy)][PF_6]$	252	577	0.369	15
$[Ir(\mathbf{7})_2(bpy)][PF_6]$	262	493, 524	3.21	64

[a] λ_{exc} = 280 nm for complexes with **3**, **5** and **7**; 340 nm for complexes with **1**, **4** and **6**.

Table 3 Solid-state photophysical properties of $[Ir(C\hat{}N)_2(bpy)][PF_6]$ (C^N = **1**, **3**–**7**)

Complex	λ_{em}^{max} [a]/nm	λ_{exc} (for PLQY)/nm	PLQY/%
$[Ir(\mathbf{1})_2(bpy)][PF_6]$	547	269	23
$[Ir(\mathbf{3})_2(bpy)][PF_6]$	532	262	6.6
$[Ir(\mathbf{4})_2(bpy)][PF_6]$	553	260	4.9
$[Ir(\mathbf{5})_2(bpy)][PF_6]$	535	262	15
$[Ir(\mathbf{6})_2(bpy)][PF_6]$	558	252	2.6
$[Ir(\mathbf{7})_2(bpy)][PF_6]$	537	262	4.2

[a] λ_{exc} = 405 nm.

to the parent complex $[Ir(ppy)_2(bpy)][PF_6]$ which emits at 585 nm (de-aerated MeCN, 298 K),[51] $[Ir(\mathbf{1})_2(bpy)][PF_6]$ shows an emission at 557 nm, consistent with a lowering of the energy of the HOMO and widening of the HOMO–LUMO gap upon the introduction of the electron-withdrawing fluoro-groups. Replacement of F by ^{t}BuS on going from $[Ir(\mathbf{1})_2(bpy)][PF_6]$ to $[Ir(\mathbf{4})_2(bpy)][PF_6]$ results in an 11 nm red-shift in the emission, and a change from ^{t}butyl to ^{n}dodecyl sulfane gives a further 9 nm red-shift. Both sulfane complexes are blue-shifted with respect to $[Ir(ppy)_2(bpy)][PF_6]$. The three sulfone complexes exhibit almost identical solution emission spectra (Fig. 10 and Table 2) with λ_{em}^{max} blue-shifted by 92 nm with respect to $[Ir(ppy)_2(bpy)][PF_6]$.

The photoluminescence quantum yields (PLQY) and lifetimes ($\tau_{1/2}$) of the solution-state emissions should be compared with values of 14% and 0.43 μs measured for $[Ir(ppy)_2(bpy)][PF_6]$ under analogous room temperature conditions.[51] Substantial enhancement of the PLQY is observed for the most electron-withdrawing (F and SO_2R) substituents (Table 2). The value of 74% for $[Ir(\mathbf{3})_2(bpy)][PF_6]$ (SO_2Me substituents) is particularly high, and it appears that increasing the steric bulk of the alkyl substituent may be detrimental to the PLQY value. We note that if solution samples are not de-aerated, the PLQY values are dramatically reduced to values of between 2.6% for $[Ir(\mathbf{6})_2(bpy)][PF_6]$ and 5.5% for $[Ir(\mathbf{5})_2(bpy)][PF_6]$, consistent with strong quenching of the phosphorescence by oxygen.

The emission lifetimes for the six complexes in de-aerated MeCN were measured under argon and are given in Table 2. The longest lived emission (3.36 μs) is for $[Ir(\mathbf{5})_2(bpy)][PF_6]$; in general, the complexes in which the cyclometallated ligand bears a sulfone substituent exhibit lifetimes that are an order of magnitude longer than those containing fluoro or sulfane group.

Fig. 11 illustrates the emission spectra of powdered samples of the complexes and emission maxima and PLQY values are given in Table 3. All emission bands are broad and featureless. For the complexes containing the sulfane- or fluoro-substituted C^N ligands (**4**, **6** or **1**), a blue shift in the emission is observed on going from solution to the solid state. For $[Ir(\mathbf{3})_2(bpy)][PF_6]$, $[Ir(\mathbf{5})_2(bpy)][PF_6]$ and $[Ir(\mathbf{7})_2(bpy)][PF_6]$, the solid-state emission maximum is red-shifted to ≈535 nm. With the exception of $[Ir(\mathbf{1})_2(bpy)][PF_6]$ for which the solid-state PLQY is 23% (λ_{exc} = 269 nm), PLQYs for powdered samples are significantly lower than those obtained in de-aerated solution (compare Tables 2 and 3).

Table 4 Cyclic voltammetric data with respect to Fc/Fc^+ in MeCN solutions with $[^tBu_4N][PF_6]$ as supporting electrolyte, and a scan rate of 0.1 V s^{-1} (ir = irreversible; qr = quasi-reversible)

Complex	$E^{ox}_{1/2}$/V	$E^{red}_{1/2}$/V	$\Delta E_{1/2}$/V
$[Ir(\mathbf{1})_2(bpy)][PF_6]$	$+1.07^{qr}$	-1.74, -2.41^{ir}, -2.54	2.81
$[Ir(\mathbf{3})_2(bpy)][PF_6]$	+1.18	-1.72, -2.16, -2.61^{ir}	2.90
$[Ir(\mathbf{4})_2(bpy)][PF_6]$	$+1.04^{ir}$	-1.75, -2.48^{ir}, -2.57^{ir}	2.79
$[Ir(\mathbf{5})_2(bpy)][PF_6]$	+1.19	-1.73, -2.18, -2.43	2.92
$[Ir(\mathbf{6})_2(bpy)][PF_6]$	$+0.82^{ir}$	-1.76, -2.55^{ir}	2.79
$[Ir(\mathbf{7})_2(bpy)][PF_6]$	+1.25	-1.71, -2.16, -2.39	2.96

Electrochemistry

Each of the $[Ir(C\text{^}N)_2(bpy)][PF_6]$ complexes (C^N = **1**, **3**–**7**) is electrochemically active, and cyclic voltammetric data are given in Table 4. Unless stated otherwise, the electrochemical processes are reversible or near-reversible. Each fluoro or sulfone derivative (C^N = **1**, **3**, **5**, **7**) exhibits an iridium-based reversible or quasi-reversible oxidation process at more positive potential than $[Ir(ppy)_2(bpy)][PF_6]$ ($E^{ox}_{1/2}$ = +0.84 V *versus* internal Fc/Fc^+),[51] consistent with the introduction of strongly electron-withdrawing substituents on the cyclometallated ligands. Compounds $[Ir(\mathbf{4})_2(bpy)][PF_6]$ and $[Ir(\mathbf{6})_2(bpy)][PF_6]$ also undergo irreversible oxidations at +1.04 and +0.82 V, respectively, which we have not investigated in detail. Two or three ligand-based reductions are observed for each complex, and the $E^{red}_{1/2}$ potentials in Table 4 compare with −1.77 and −2.60 V for $[Ir(ppy)_2(bpy)][PF_6]$.[51] The LUMO is localized on the bpy ligand,[1] and the values of the reduction potentials are consistent with the processes being bpy-based, being little affected by the electronic changes made to the C^N ligand across the series of compounds.

The electrochemical band gaps, $\Delta E_{1/2}$ (Table 4) are all larger than the 2.61 V in $[Ir(ppy)_2(bpy)][PF_6]$,[51] consistent with the lowering of the HOMO upon introducing electron-withdrawing substituents into the C^N domain. As expected, the largest band gaps are observed for the sulfone derivatives (C^N = **3**, **5**, **7**). The trends in Table 4 parallel those observed in the solution emission spectra (Table 2). The slightly smaller values of $\Delta E_{1/2}$ on going from fluoro to sulfane derivatives are consistent with the observed red-shift in emission maxima, while the increase in $\Delta E_{1/2}$ on going to sulfones $[Ir(C\text{^}N)_2(bpy)][PF_6]$ (C^N = **3**, **5**, **7**) corresponds to the blue-shift in the emissions compared to those of $[Ir(C\text{^}N)_2(bpy)][PF_6]$ (C^N = **1**, **4**, **6**).

Conclusions

We have prepared a series of $[Ir(C\text{^}N)_2(bpy)][PF_6]$ complexes in which the cyclometallating ligands contain electron-withdrawing fluoro, sulfane or sulfone groups. The well-established synthetic route of treatment of a $[Ir_2(C\text{^}N)_4Cl_2]$ dimer with the bpy proved appropriate for the preparation of $[Ir(C\text{^}N)_2(bpy)][PF_6]$ with C^N = **1**, **3**, **4**, **5** and **7**. However, $[Ir(\mathbf{6})_2(bpy)][PF_6]$ was prepared by nucleophilic substitution starting from fluoro-derivative $[Ir(\mathbf{1})_2(bpy)][PF_6]$ since attempts to prepare the dimer $[Ir_2(\mathbf{6})_4Cl_2]$ were unsuccessful.

The new complexes have been fully characterized by spectroscopic and mass spectrometric methods. The single crystal structures of Δ-$[Ir(\mathbf{1})_2(bpy)][PF_6]$ and of *rac*-4{$[Ir(\mathbf{1})_2(bpy)][PF_6]$}·$Et_2O$·$2CH_2Cl_2$ have been elucidated, along with the structures of the free ligands H**3** and H**5**, and of the dimer $[Ir_2(\mathbf{3})_4Cl_2]$·$2CH_2Cl_2$. The solution absorption spectra of the complexes are dominated by ligand-centred transitions, with a tail into the visible arising from low intensity ^{1}MLCT and ^{1}LLCT bands. The room temperature, solution emission spectra of $[Ir(\mathbf{1})_2(bpy)][PF_6]$, $[Ir(\mathbf{4})_2(bpy)][PF_6]$ and $[Ir(\mathbf{6})_2(bpy)][PF_6]$ (fluoro and sulfane substituents) are broad and featureless, consistent with substantial CT contributions to the lowest energy triplet (emitting) state. These complexes are all yellow emitters with λ^{max}_{em} between 557 and 577 nm. In contrast, incorporation of the sulfone substituents into the cyclometallating ligands results in $[Ir(\mathbf{3})_2(bpy)][PF_6]$, $[Ir(\mathbf{5})_2(bpy)][PF_6]$ and $[Ir(\mathbf{7})_2(bpy)][PF_6]$ being green emitters which exhibit structured emissions (λ^{max}_{em} = 493 and 523 to 525 nm), consistent with only minor CT contributions to the lowest energy triplet state. The solution PLQYs of the sulfone complexes are 74% for $[Ir(\mathbf{3})_2(bpy)][PF_6]$ and 64% for both $[Ir(\mathbf{5})_2(bpy)][PF_6]$ and $[Ir(\mathbf{7})_2(bpy)][PF_6]$, but for powdered solid samples, these are significantly lower (≤15%). The emission lifetimes for the complexes containing sulfone substituents in the C^N ligands (**3**, **5** and **7**) are an order of magnitude longer (2.33 to 3.36 μs) than the complexes in which the C^N ligand carries a fluoro or sulfane unit (0.224 to 0.528 μs). We are currently screening $[Ir(\mathbf{3})_2(bpy)][PF_6]$, $[Ir(\mathbf{5})_2(bpy)][PF_6]$ and $[Ir(\mathbf{7})_2(bpy)][PF_6]$ and related complexes in device configuration in LECs.

Acknowledgements

We thank the Swiss National Science Foundation, the European Research Council (Advanced Grant 267816 LiLo) and the University of Basel for financial support.

Notes and references

1 R. D. Costa, E. Ortí, H. J. Bolink, F. Monti, G. Accorsi and N. Armaroli, *Angew. Chem., Int. Ed.*, 2012, **51**, 8178.
2 T. Hu, L. He, L. Duan and Y. Qiu, *J. Mater. Chem.*, 2012, **22**, 4206.
3 F. Dumar, D. Bertin and D. Gigmes, *Int. J. Nanotechnol.*, 2012, **9**, 377.
4 R. D. Costa, in *Molecules at Work*, ed. B. Pignataro, Wiley-VCH, Weinheim, 2012, pp. 339–360.
5 N. M. Shavaleev, R. Scopelliti, M. Grätzel and Md. K. Nazeeruddin, *Inorg. Chim. Acta*, 2013, **396**, 17.
6 N. M. Shavaleev, F. Monti, R. D. Costa, R. Scopelliti, H. J. Bolink, E. Ortí, G. Accorsi, N. Armaroli, E. Baranoff, M. Grätzel and Md. K. Nazeeruddin, *Inorg. Chem.*, 2012, **51**, 2263.

7 T. Kim, H. Kim, K. M. Lee, Y. S. Lee and M. H. Lee, *Inorg. Chem.*, 2012, **52**, 160.
8 D. Tordera, J. J. Serrano-Pérez, A. Pertegás, E. Ortí, H. J. Bolink, E. Baranoff, Md. K. Nazeeruddin and J. Frey, *Chem. Mater.*, 2013, **25**, 3391.
9 G. Zhou, Q. Wang, C.-L. Ho, W.-Y. Wong, D. Ma, L. Wang and Z. Lin, *Chem.–Asian J.*, 2008, **3**, 1830.
10 G. Zhou, C.-L. Ho, W.-Y. Wong, Q. Wang, D. Ma, L. Wang, Z. Lin, T. B. Marder and A. Beeby, *Adv. Funct. Mater.*, 2008, **18**, 499.
11 R. Ragni, E. Orselli, G. S. Kottas, O. H. Omar, F. Babudri, A. Pedone, F. Naso, G. M. Farinola and L. De Cola, *Chem.–Eur. J.*, 2009, **15**, 136.
12 M. Tavasli, S. Bettington, I. F. Perepichka, A. S. Batsanov, M. R. Bryce, C. Rothe and A. P. Monkman, *Eur. J. Inorg. Chem.*, 2007, 4808.
13 D. Tordera, A. M. Bünzli, A. Pertegás, J. M. Junquera-Hernández, E. C. Constable, J. A. Zampese, C. E. Housecroft, E. Ortí and H. J. Bolink, *Chem.–Eur. J*, 2013, **19**, 8597.
14 I. Bouamaied, E. C. Constable, C. E. Housecroft, M. Neuburger and J. A. Zampese, *Dalton Trans.*, 2012, **41**, 10276.
15 C. Hansch, A. Leo and R. W. Taft, *Chem. Rev.*, 1991, **91**, 165.
16 J. Chambers, B. Eaves, D. Parker, R. Claxton, P. S. Ray and S. J. Slattery, *Inorg. Chim. Acta*, 2006, **359**, 2400.
17 D. H. McDaniel and H. C. Brown, *J. Org. Chem.*, 1958, **23**, 420.
18 E. C. Constable, A. M. W. Cargill Thompson, N. Armaroli, V. Balzani and M. Maestri, *Polyhedron*, 1992, **11**, 2707.
19 C. Liu, Q. Ni, P. Hu and J. Qiu, *Org. Biomol. Chem.*, 2011, **9**, 1054.
20 L. Ackermann, H. K. Potukuchi, A. R. Kapdi and C. Schulzke, *Chem.–Eur. J.*, 2010, **16**, 3300.
21 J. Xu, G. Cheng, D. Su, Y. Liu, X. Wang and Y. Hu, *Chem.–Eur. J.*, 2009, **15**, 13105.
22 M. Marigo, N. Marsich and E. Farnetti, *J. Mol. Catal. A: Chem.*, 2002, **187**, 169.
23 Y. Harrak, G. Casula, J. Basset, G. Rosell, S. Plescia, D. Raffa, M. G. Cusimano, R. Pouplana and M. D. Pujol, *J. Med. Chem.*, 2010, **53**, 6560.
24 *APEX2, version 2 User Manual, M86-E01078*, Bruker Analytical X-ray Systems, Inc., Madison, WI, 2006.
25 G. M. Sheldrick, *Acta Crystallogr., Sect. A: Fundam. Crystallogr.*, 2008, **64**, 112.
26 I. J. Bruno, J. C. Cole, P. R. Edgington, M. K. Kessler, C. F. Macrae, P. McCabe, J. Pearson and R. Taylor, *Acta Crystallogr., Sect. B: Struct. Sci.*, 2002, **58**, 389.
27 C. F. Macrae, I. J. Bruno, J. A. Chisholm, P. R. Edgington, P. McCabe, E. Pidcock, L. Rodriguez-Monge, R. Taylor, J. van de Streek and P. A. Wood, *J. Appl. Crystallogr.*, 2008, **41**, 466.
28 S. Clavier, Ø. Rist, S. Hansen, L.-O. Gerlach, T. Högberg and J. Bergman, *Org. Biomol. Chem.*, 2003, **1**, 4248.
29 A. B. Charette, C. Berthelette and D. St-Martin, *Tetrahedron Lett.*, 2001, **42**, 5149.
30 F. A. M. Rudolph, A. L. Fuller, A. M. Z. Slawin, M. Bühl, R. A. Aitken and J. D. Woollins, *J. Chem. Crystallogr.*, 2010, **40**, 253 and references therein.
31 C. Glidewell, W. T. A. Harrison, J. N. Low, J. G. Sime and J. L. Wardell, *Acta Crystallogr., Sect. B: Struct. Sci.*, 2001, **57**, 190.
32 See for example: F. Neve, A. Crispini, S. Campagna and S. Serroni, *Inorg. Chem.*, 1999, **38**, 2250.
33 S. Sprouse, K. A. King, P. J. Spellane and R. J. Watts, *J. Am. Chem. Soc.*, 1984, **106**, 6647.
34 F. O. Garces, K. A. King and R. J. Watts, *Inorg. Chem.*, 1988, **27**, 3464.
35 E. Baranoff, B. F. E. Curchod, J. Frey, R. Scopelliti, F. Kessler, I. Tavernelli, U. Rothlisberger, M. Grätzel and Md. K. Nazeeruddin, *Inorg. Chem.*, 2012, **51**, 215.
36 F. H. Allen, *Acta Crystallogr., Sect. B: Struct. Sci.*, 2002, **58**, 380.
37 E. Andreiadis, D. Imbert, J. Pécaut, A. Calborean, I. Ciofini, C. Adamo, R. Demadrille and M. Mazzanti, *Inorg. Chem.*, 2011, **50**, 8197.
38 S. Bettington, M. Tavasli, M. R. Bryce, A. S. Batsanov, A. L. Thompson, H. A. Al Attar, F. B. Dias and A. P. Monkman, *J. Mater. Chem.*, 2006, **16**, 1046.
39 S. Bettington, A. L. Thompson, A. Beeby and A. E. Goeta, *Acta Crystallogr., Sect. E: Struct. Rep. Online*, 2004, **60**, m827.
40 C. Xu, Z.-Q. Wang, X.-M. Dong, X.-Q. Hao, X.-M. Zhao, B.-M. Ji and M.-P. Song, *Inorg. Chim. Acta*, 2001, **373**, 306.
41 K. A. McGee and K. R. Mann, *Inorg. Chem.*, 2007, **46**, 7800.
42 O. Chepelin, J. Ujma, X. Wu, A. M. Z. Slawin, M. B. Pitak, S. J. Coles, J. Michel, A. C. Jones, P. E. Barran and P. J. Lusby, *J. Am. Chem. Soc.*, 2012, **134**, 19334.
43 F. O. Garces, K. Dedeian, N. L. Keder and R. J. Watts, *Acta Crystallogr., Sect. C: Cryst. Struct. Commun.*, 1993, **49**, 1117.
44 L. Norel, M. Rudolph, N. Vanthuyne, J. A. G. Williams, C. Lescop, C. Roussel, J. Autschbach, J. Crassous and R. Réau, *Angew. Chem., Int. Ed.*, 2010, **49**, 99.
45 E. Baranoff, H. J. Bolink, E. C. Constable, M. Delgado, D. Häussinger, C. E. Housecroft, M. K. Nazeeruddin, M. Neuburger, E. Ortí, G. E. Schneider, D. Tordera, R. M. Walliser and J. A. Zampese, *Dalton Trans.*, 2013, **42**, 1073.
46 G. E. Schneider, H. J. Bolink, E. C. Constable, C. D. Ertl, C. E. Housecroft, A. Pertegàs, J. A. Zampese, A. Kanitz, F. Kessler and S. B. Meier, *Dalton Trans.*, 2014, **43**, 1961.
47 I. Dance and M. Scudder, *J. Chem. Soc., Dalton Trans.*, 1998, 1341.
48 A. Forni, S. Pieraccini, S. Rendine, F. Gabas and M. Sironi, *ChemPhysChem*, 2012, **13**, 4224.
49 See for example: J. Ganifo, D. Toledo, M. T. Garland and R. Baggio, *J. Fluorine Chem.*, 2010, **131**, 510.
50 C. Janiak, *J. Chem. Soc., Dalton Trans.*, 2000, 3885.
51 R. D. Costa, E. Ortí, D. Tordera, A. Pertegás, H. J. Bolink, S. Graber, C. E. Housecroft, L. Sachno, M. Neuberger and E. C. Constable, *Adv. Energy Mater.*, 2011, **1**, 282.

